

## WELL-POSED BOUNDARY INTEGRAL EQUATION FORMULATIONS AND NYSTRÖM DISCRETIZATIONS FOR THE SOLUTION OF HELMHOLTZ TRANSMISSION PROBLEMS IN TWO-DIMENSIONAL LIPSCHITZ DOMAINS

VÍCTOR DOMÍNGUEZ, MARK LYON AND CATALIN TURC

Communicated by Francisco-Javier Sayas

**ABSTRACT.** We present a comparison among the performance of solvers based on Nyström discretizations of several well-posed boundary integral equation formulations of Helmholtz transmission problems in two-dimensional Lipschitz domains. Specifically, we focus on the following four classes of boundary integral formulations of Helmholtz transmission problems: (1) the classical first kind integral equations for transmission problems [13], (2) the classical second kind integral equations for transmission problems [25], (3) the *single* integral equation formulations [21], and (4) certain *direct* counterparts of recently introduced generalized combined source integral equations [4, 5]. The former two formulations were the only formulations whose well-posedness in Lipschitz domains was rigorously established [13, 36]. We establish the well-posedness of the latter two formulations in appropriate functional spaces of boundary traces of solutions of transmission Helmholtz problems in Lipschitz domains. We give ample numerical evidence that Nyström solvers based on formulations (3) and (4) are computationally more advantageous than solvers based on the classical formulations (1) and (2), especially in the case of high-contrast transmission problems at high frequencies.

---

2010 AMS *Mathematics subject classification.* Primary 35J05, 65F08, 65N38, 65T40.

*Keywords and phrases.* Transmission problems, integral equations, Lipschitz domains, regularizing operators, Nyström method, graded meshes.

The first author was partially supported by Ministerio de Economía y Competitividad, grant No. MTM2014-52859. The third author gratefully acknowledges support from NSF grant No. DMS-1312169.

Received by the editors on September 15, 2015, and in revised form on May 11, 2016.

**1. Introduction.** A wide variety of well-posed boundary integral equations for the solution of Helmholtz transmission problems has been proposed in the literature, at least in the case when the interfaces of material discontinuity are regular enough. Most of these formulations are derived from representations of the fields in each region filled by a homogeneous material by suitable combinations of single and double layer potentials. The enforcement of the continuity of solutions and their normal derivatives across interfaces of material discontinuity leads to combined field integral equations (CFIE) of transmission scattering problems. Some of these integral formulations involve two unknowns [13, 20, 25, 32, 34] or three or more unknowns [27, 33], while others involve one unknown per each interface of material discontinuity [21]. It is also possible to formulate transmission problems in terms of both interior and exterior traces-multi-trace formulations (MTF), that is, using four unknowns per each interface of material discontinuity [11, 18]. More general boundary problems, which include not only transmission conditions but mixed Dirichet-Neumann conditions in complex geometrical configurations as well, have been studied in [38].

In the technologically important case of transmission problems at high-frequencies, the numerical solutions of boundary integral equation formulations typically rely on Krylov subspace iterative methods. As in the case of impenetrable scattering problems [6], the classical boundary integral equations of transmission problems are not particularly well suited for Krylov iterative solutions of transmission problems at high-frequencies. We have recently demonstrated that a novel class of boundary integral equations, referred to as generalized combined source integral equations (GCSIE) [4, 5] is a more favorable alternative for smooth transmission problems that involve high-contrast configurations at high-frequencies. The main scope of this paper is to investigate to what extent the aforementioned claim is valid in the case of high-frequency, high-contrast Helmholtz transmission problems when the interface of material continuity is a Lipschitz curve.

An important question related to boundary integral equation (BIE) formulations of linear, constant-coefficient PDEs is whether the BIE are well-posed. This issue is typically settled via Fredholm arguments whose flavor differ significantly from the case of regular boundaries to the case of Lipschitz boundaries. The case of smooth boundaries is

extremely well understood and researched, as one can take full advantage of the increased smoothing properties of double layer operators that guarantee compactness properties needed in the Fredholm theory [5]. In addition, a very general methodology based on coercive approximations of Dirichlet-to-Neumann operators can deliver optimally conditioned boundary integral formulations (GCSIE) for transmission Helmholtz problems [5]; the aforementioned enhanced smoothing properties play a major role in establishing the well-posedness of the GCSIE in the smooth case. We address in this paper the issues of well-posedness and well-conditioning of the GCSIE formulations in the Lipschitz case by making use of deep results from harmonic analysis [37] and certain duality pairings. We also present a *direct* counterpart to the GCSIE formulations which we refer to as regularized combined field integral equations (CFIER). From the numerical point of view the main advantage of direct CFIER formulations is given by the fact that they employ as unknowns Dirichlet and Neumann traces of transmission problems, whose singular behavior around corner points is well understood [13] and thus can be resolved by graded meshes towards corners. This brings us to the second major point of this paper, high-order Nyström discretizations of transmission boundary integral equations in two-dimensional Lipschitz domains.

High-order Nyström methods typically employ graded meshes in order to deal with singularities associated with solutions of boundary integral equations in domains with corners [16, 17, 22]. One issue that arises in this regard is the possibly unbounded nature of such solutions in the neighborhood of corners in the case of integral formulations of the second kind. While in several instances the issue can be avoided by resorting to alternative integral equation formulations [2] whose solutions are regular enough (e.g., Hölder continuous), in many others, including the case of transmission problems in domains with corners, the unboundedness of solutions cannot be avoided. Two main approaches to tackle the unbounded nature of solutions of integral equations of the second kind have recently been introduced: (a) one that relies on incorporation of the *known* asymptotic infinite behavior of solutions in the vicinity of corners and exact cancellations of infinite quantities [9]; and (b) one that uses Jacobians associated with graded meshes in order to introduce more regular *weighted* solutions as new unknowns of newly weighted integral formulations of the second kind [8, 15, 19, 28, 31].

We pursue a version of the latter approach in this paper in conjunction with simple modifications of a Nyström method based on global trigonometric interpolation, singular kernel-splitting, and analytic evaluations of integrals that involve products of certain singular functions and Fourier harmonics [26, 29]. Several ideas in this approach were introduced in [28] for the discretization of the first kind boundary integral equation formulation of transmission problems [13] in domains with corners. The method incorporates sigmoid transforms [22] within parametrizations of domains with corners, and it uses the Jacobians of these transformations as multiplicative weights to define new unknowns.

Specifically, the focus of the paper is on direct integral formulations of transmission problems whereby the unknowns are the Dirichlet and Neumann traces of solutions of transmission problems on the Lipschitz boundary. A weighted Neumann trace defined as the product of the derivatives of the sigmoid parametrizations and the usual Neumann trace of solution of transmission problems is introduced as a new unknown; given that the derivatives of the parametrizations that incorporate sigmoid transforms vanish polynomially at corners, the weighted traces are more regular for large enough values of the order of the polynomial in the sigmoid transform. Introducing new weighted unknowns also requires definitions of new weighted boundary integral equations that involve weighted versions of the four scattering boundary integral operators. It turns out that the kernel splitting techniques originally developed for smooth curves [23] can be easily extended to weighted boundary integral operators, delivering a high-order Nyström discretizations for the various formulations considered in this paper. We give ample numerical evidence that, in the high-contrast, high-frequency regime, the single integral equation formulations and our novel regularized formulations have superior spectral properties over the classical formulations of transmission problems, giving rise to important computational savings.

The paper is organized as follows. In Section 2, we formulate the Helmholtz transmission problem we are interested in. In Section 3, we recount the definition of the four scattering boundary integral operators, and we discuss several boundary integral formulations of the Helmholtz transmission problem. In Section 4, we establish the well-posedness of several of the boundary integral formulations discussed in

this paper, including the regularized formulations CFIER; finally, in Section 5, we present high-order Nyström discretizations of the various boundary integral equations considered in this paper, and we carry out a comparison between solvers based on these formulations that emphasizes the benefits that can be garnered from the use of single integral equations and regularized integral equations.

## 2. Integral equations of Helmholtz transmission problems.

We consider the problem of evaluating the time-harmonic fields  $u^1$  and  $u^2$  that result as an incident field  $u^{\text{inc}}$  impinges upon the boundary  $\Gamma$  of a homogeneous dielectric scatterer  $D_2$  which occupies a bounded region in  $\mathbb{R}^2$ . We assume that both media occupying  $D_2$  and its exterior are nonmagnetic, and the electric permittivity of the dielectric material inside the domain  $D_2$  is denoted by  $\epsilon_2$  while that of the medium occupying the exterior of  $D_2$  is denoted by  $\epsilon_1$ . The frequency domain dielectric transmission problem is formulated in terms of finding fields  $u^1$  and  $u^2$  that are solutions to the Helmholtz equations:

$$(2.1) \quad \begin{aligned} \Delta u^2 + k_2^2 u^2 &= 0, & \text{in } D_2, \\ \Delta u^1 + k_1^2 u^1 &= 0, & \text{in } D_1 = \mathbb{R}^2 \setminus \overline{D_2}, \end{aligned}$$

where the wavenumbers  $k_i$ ,  $i = 1, 2$ , are defined as  $k_i = \omega \sqrt{\epsilon_i}$ ,  $i = 1, 2$ , in terms of the frequency  $\omega$ . The incident field  $u^{\text{inc}}$  is assumed to satisfy

$$(2.2) \quad \Delta u^{\text{inc}} + k_1^2 u^{\text{inc}} = 0 \quad \text{in } \tilde{D}_2,$$

where  $\tilde{D}_2$  is an open neighborhood of  $\overline{D_2}$ . Therefore,  $u^{\text{inc}}$  has to be smooth, actually analytic, in  $\overline{D_2}$ , which includes plane waves or spherical waves from a point source placed in the exterior domain  $D_1$ .

In addition, the fields  $u^1$ ,  $u^{\text{inc}}$ , and  $u^2$  are related on the boundary  $\Gamma$  by the following boundary conditions

$$(2.3) \quad \begin{aligned} \gamma_D^1 u^1 + \gamma_D u^{\text{inc}} &= \gamma_D^2 u^2 & \text{on } \Gamma \\ \gamma_N^1 u^1 + \gamma_N u^{\text{inc}} &= \rho \gamma_N^2 u^2 & \text{on } \Gamma \end{aligned}$$

with  $\rho > 0$ . In equations (2.3) and what follows  $\gamma_D^i$ ,  $i = 1, 2$ , denote exterior ( $i = 1$ ) and interior Dirichlet traces ( $i = 2$ ). Similarly  $\gamma_N^i$ ,  $i = 1, 2$ , denote exterior and interior Neumann traces taken with respect to the exterior unit normal on  $\Gamma$ . When both Dirichlet, respectively Neumann, traces coincide, we will simply write  $\gamma_D$ , respectively  $\gamma_N$ .

(Notice that  $\gamma_D^1 u^{\text{inc}} = \gamma_D^2 u^{\text{inc}}$ ,  $\gamma_N^1 u^{\text{inc}} = \gamma_N^2 u^{\text{inc}}$ , and therefore, we are allowed to use  $\gamma_{\{D,N\}} u^{\text{inc}}$  in (2.3).)

We assume in what follows that the boundary  $\Gamma$  is a closed Lipschitz curve in  $\mathbb{R}^2$ . Depending on the type of scattering problem, the transmission coefficient  $\rho$  in equations (2.3) can be either 1 (E-polarized) or  $\epsilon_1/\epsilon_2$  (H-polarized). We furthermore require that  $u^1$  satisfies the Sommerfeld radiation conditions at infinity:

$$(2.4) \quad \lim_{|\mathbf{r}| \rightarrow \infty} |\mathbf{r}|^{1/2} (\partial u^1 / \partial \mathbf{r} - ik_1 u^1) = 0.$$

(Here  $\partial/\partial \mathbf{r}$  is the radial derivative.) Note that, under these assumptions, the wavenumbers  $k_i$ ,  $i = 1, 2$ , are real numbers. It is well known that, in this case, the systems of partial differential equations (2.1)–(2.2) together with the boundary conditions (2.3) and the radiation condition (2.4) has a unique solution [21, 25]. The results here can be extended to the case of complex wavenumbers  $k_i$ ,  $i = 1, 2$ , provided we assume uniqueness of the transmission problem and its adjoint, that is, for the same transmission problem but with wavenumbers  $k_1$  for  $D_2$  and  $k_2$  for  $D_1$  [25].

**3. Boundary integral formulation for transmission problems.** A variety of well-posed integral equations for the transmission problems (2.1)–(2.3) exist [4, 13, 21, 25]. On one hand, integral equation formulations for transmission problems can be formulated as a  $2 \times 2$  system of integral equations which can be derived from (a) Green’s formulas in both domains  $D_1$  and  $D_2$ , in which case they are referred to as *direct* integral equation formulations [13, 21], (b) from representations of the fields  $u^j$ ,  $j = 1, 2$ , in forms of suitable combinations of single and double layer potentials in both domains  $D_1$  and  $D_2$ , in which case they are referred to as *indirect* integral equation formulations [25], or (c) from Green’s formulas and suitable approximations to exterior and interior Dirichlet-to-Neumann operators, in which case they are referred to as *regularized* combined field integral equations or generalized combined source integral equations [4]. On the other hand, integral equation formulations for transmission problems can be formulated as *single* integral equations which can be derived from (d) Green’s formulas in one of the domains and (indirect) combined field representations in the other domain [21]. The strategies recounted above lead to Fredholm second kind boundary integral equations for the solution

of transmission problems [4, 5, 21, 25], at least in the case when the curve  $\Gamma$  is smooth enough ( $C^3$  suffices). The first part of this paper is devoted to establishing the well-posedness of the boundary integral equations of types (c) and (d) in the case when the curve  $\Gamma$  is Lipschitz. To this end, we begin by reviewing the definition and mapping properties of the various scattering boundary integral operators.

**3.1. Layer potentials and operators.** We start with the definitions of *single* and *double layer potentials*. Given a wavenumber  $k$  such that  $\Re k > 0$  and  $\Im k \geq 0$ , and a density  $\varphi$  defined on  $\Gamma$ , we define the single layer potential as

$$[SL_k(\varphi)](\mathbf{z}) := \int_{\Gamma} G_k(\mathbf{z} - \mathbf{y})\varphi(\mathbf{y}) ds(\mathbf{y}), \quad \mathbf{z} \in \mathbb{R}^2 \setminus \Gamma,$$

and the double layer potential as

$$[DL_k(\varphi)](\mathbf{z}) := \int_{\Gamma} \frac{\partial G_k(\mathbf{z} - \mathbf{y})}{\partial \mathbf{n}(\mathbf{y})} \varphi(\mathbf{y}) ds(\mathbf{y}), \quad \mathbf{z} \in \mathbb{R}^2 \setminus \Gamma,$$

where  $G_k(\mathbf{x}) = (i/4)H_0^{(1)}(k|\mathbf{x}|)$  represents the two-dimensional Green's function of the Helmholtz equation with wavenumber  $k$ . The Dirichlet and Neumann exterior and interior traces on  $\Gamma$  of the single and double layer potentials corresponding to the wavenumber  $k$  and a density  $\varphi$  are given by:

$$\begin{aligned} \gamma_D^1 SL_k(\varphi) &= \gamma_D^2 SL_k(\varphi) = \gamma_D SL_k(\varphi) = S_k \varphi \\ \gamma_N^j SL_k(\varphi) &= (-1)^j \frac{\varphi}{2} + K_k^\top \varphi, \quad j = 1, 2 \\ \gamma_D^j DL_k(\varphi) &= (-1)^{j+1} \frac{\varphi}{2} + K_k \varphi, \quad j = 1, 2 \\ \gamma_N^1 DL_k(\varphi) &= \gamma_N^2 DL_k(\varphi) = \gamma_N DL_k(\varphi) = \varphi. \end{aligned} \tag{3.1}$$

In equations (3.1), the operators  $K_k$  and  $K_k^\top$ , usually referred to as double and adjoint double layer operators, are defined for a given wavenumber  $k$  and density  $\varphi$  as

$$(K_k \varphi)(\mathbf{x}) := \int_{\Gamma} \frac{\partial G_k(\mathbf{x} - \mathbf{y})}{\partial \mathbf{n}(\mathbf{y})} \varphi(\mathbf{y}) ds(\mathbf{y}), \quad \mathbf{x} \text{ on } \Gamma \tag{3.2}$$

and

$$(K_k^\top \varphi)(\mathbf{x}) := \int_{\Gamma} \frac{\partial G_k(\mathbf{x} - \mathbf{y})}{\partial \mathbf{n}(\mathbf{x})} \varphi(\mathbf{y}) ds(\mathbf{y}), \quad \mathbf{x} \text{ on } \Gamma. \tag{3.3}$$

Furthermore, for a given wavenumber  $k$  and density  $\varphi$ , the operator  $N_k$  denotes the Neumann trace of the double layer potential on  $\Gamma$  given in terms of a Hadamard finite part (FP) integral which can be re-expressed in terms of a Cauchy principal value (PV) integral that involves the tangential derivative  $\partial_s$  on the curve  $\Gamma$

$$\begin{aligned}
 (3.4) \quad (N_k\varphi)(\mathbf{x}) &:= \text{FP} \int_{\Gamma} \frac{\partial^2 G_k(\mathbf{x} - \mathbf{y})}{\partial \mathbf{n}(\mathbf{x}) \partial \mathbf{n}(\mathbf{y})} \varphi(\mathbf{y}) \, ds(\mathbf{y}) \\
 &= k^2 \int_{\Gamma} G_k(\mathbf{x} - \mathbf{y})(\mathbf{n}(\mathbf{x}) \cdot \mathbf{n}(\mathbf{y})) \varphi(\mathbf{y}) \, ds(\mathbf{y}) \\
 &\quad + \text{PV} \int_{\Gamma} \partial_s G_k(\mathbf{x} - \mathbf{y}) \partial_s \varphi(\mathbf{y}) \, ds(\mathbf{y}).
 \end{aligned}$$

Finally, the single layer operator  $S_k$  is defined for a wavenumber  $k$  as

$$(3.5) \quad (S_k\varphi)(\mathbf{x}) := \int_{\Gamma} G_k(\mathbf{x} - \mathbf{y}) \varphi(\mathbf{y}) \, ds(\mathbf{y}), \quad \mathbf{x} \text{ on } \Gamma$$

for a density function  $\varphi$  defined on  $\Gamma$ .

We commit here another slight abuse of notation and denote  $SL_1, DL_1, S_1, N_1, \dots$ , in what follows for layer potentials and operators corresponding to  $k_1$ , that is,

$$SL_1 = SL_{k_1} \quad DL_1 = DL_{k_1}, \quad S_1 = S_{k_1}, \dots$$

Analogously,

$$SL_2 = SL_{k_2} \quad DL_2 = DL_{k_2}, \quad S_2 = S_{k_2}, \dots$$

We stress that the context will avoid any possible confusion between indices and wavenumbers. This convention helps us to enhance and lighten the notation. Notice that Green identities can now be written in the simple form:

$$(3.6) \quad u^j = (-1)^j SL_j(\gamma_N^j u^j) - (-1)^j DL_j(\gamma_D^j u^j).$$

Similarly,

$$(3.7) \quad C_j = \frac{1}{2} \begin{bmatrix} I & \\ & I \end{bmatrix} + (-1)^j \begin{bmatrix} -K_j & S_j \\ -N_j & K_j^T \end{bmatrix}, \quad j = 1, 2,$$

are the exterior/interior Calderón projections associated to the exterior/interior Helmholtz equation:

$$(3.8) \quad C_j^2 = C_j, \quad C_j \begin{bmatrix} \gamma_D^j u^j \\ \gamma_N^j u^j \end{bmatrix} = \begin{bmatrix} \gamma_D^j u^j \\ \gamma_N^j u^j \end{bmatrix}.$$

We recall that from (3.7) and (3.8) one easily deduces

$$(3.9) \quad \begin{aligned} S_k N_k &= -\frac{1}{4}I + K_k^2, \\ N_k S_k &= -\frac{1}{4}I + (K_k^\top)^2, \\ N_k K_k &= K_k^\top N_k, \\ K_k S_k &= S_k K_k^\top. \end{aligned}$$

We end this section by noting that, since  $u^{\text{inc}}$  solves  $\Delta v + k_1^2 v = 0$  in  $D_2$ , the following holds:

$$(3.10) \quad C_1 \begin{bmatrix} \gamma_D u^{\text{inc}} \\ \gamma_N u^{\text{inc}} \end{bmatrix} = \mathbf{0},$$

and therefore,

$$(3.11) \quad -SL_1(\gamma_N u^{\text{inc}}) + DL_1(\gamma_D u^{\text{inc}}) = 0, \quad \text{in } D_1.$$

**3.2. Boundary integral equations.** Let us first introduce the total field given by

$$(3.12) \quad u^t = \begin{cases} u^1 + u^{\text{inc}} & \text{in } D_1 \\ u^2 & \text{in } D_2. \end{cases}$$

The unknowns in the direct formulations considered in this paper are

$$(3.13) \quad \gamma_D u^t = \gamma_D^1(u^1 + u^{\text{inc}}) = \gamma_D^2 u^2, \quad \gamma_N^1 u^t = \gamma_N^1(u^1 + u^{\text{inc}})$$

the Dirichet and Neumann data for the total field from the unbounded domain. We then construct  $u^1$  and  $u^2$  using Green’s identities (3.6). Actually, for the exterior solution, the following holds as well:

$$(3.14) \quad u^1 = -SL_1(\gamma_N^1 u^t) + DL_1(\gamma_D u^t),$$

which is a consequence of the definition of the total wave  $u^t$  and of the identity (3.11) which ensures that the contribution from  $u^{\text{inc}}$  in the representation formula cancels out.

First, we obtain the following first kind integral equations due to [13] with a positive definite principal part:

$$(3.15) \quad \text{CFK} \begin{bmatrix} \gamma_D u^t \\ \gamma_N^1 u^t \end{bmatrix} := \begin{bmatrix} -(K_1 + K_2) & (\rho^{-1} S_2 + S_1) \\ -(N_1 + \rho N_2) & (K_1^\top + K_2^\top) \end{bmatrix} \begin{bmatrix} \gamma_D u^t \\ \gamma_N^1 u^t \end{bmatrix} = \begin{bmatrix} \gamma_D u^{\text{inc}} \\ \gamma_N u^{\text{inc}} \end{bmatrix}.$$

This system of integral equations can be easily derived from (3.7)–(3.10) and the boundary conditions (2.3). Obviously, these integral equations are understood in the almost everywhere sense. We refer to the system of boundary integral equations (3.15) as CFIEFK for *combined field integral equation of the first kind*.

A widely used first kind boundary integral formulation of the transmission problems (2.1)–(2.3) is due to Kress and Roach, cf., [25], and it consists of the following pair of integral equations:

$$(3.16) \quad \text{CSK} \begin{bmatrix} \gamma_D u^t \\ \gamma_N^1 u^t \end{bmatrix} := \left( \frac{\rho^{-1} + 1}{2} \begin{bmatrix} I & \\ & I \end{bmatrix} + \begin{bmatrix} (K_2 - \rho^{-1} K_1) & \rho^{-1} (S_1 - S_2) \\ -(N_1 - N_2) & (K_1^\top - \rho^{-1} K_2^\top) \end{bmatrix} \right) \begin{bmatrix} \gamma_D u^t \\ \gamma_N^1 u^t \end{bmatrix} = \begin{bmatrix} \rho^{-1} \gamma_D u^{\text{inc}} \\ \gamma_N u^{\text{inc}} \end{bmatrix}.$$

In what follows, we refer to the integral equations (3.16) as CFIESK (*combined field integral equation of the second kind*).

We recently introduced generalized combined source integral equation (GCSIE) formulations of transmission problems [4, 5], and we established their well-posedness in the case when  $\Gamma$  is regular enough. We consider here a *direct* counterpart of the GCSIE formulations which can be obtained by combining the previous formulations in the form:

$$(3.17a) \quad \left( \frac{\rho}{\rho + 1} \text{CSK} + \frac{2}{1 + \rho} \begin{bmatrix} S_\kappa \\ -\rho N_\kappa \end{bmatrix} \text{CFK} \right) \begin{bmatrix} \gamma_D u^t \\ \gamma_N^1 u^t \end{bmatrix} = \frac{1}{\rho + 1} \begin{bmatrix} I & 2S_\kappa \\ -2\rho N_\kappa & \rho I \end{bmatrix} \begin{bmatrix} \gamma_D u^{\text{inc}} \\ \gamma_N u^{\text{inc}} \end{bmatrix}.$$

Here,  $\kappa$  is a complex wave number with positive imaginary part. This parameter can be appropriately taken to improve the spectrum of the underlying operator. This leads to faster convergence, when discretized, of Kyrlov iterative methods, such as GMRES, for the linear system (see subsection 5.4). Defining

$$R := \frac{1}{\rho + 1} \begin{bmatrix} I & 2S_\kappa \\ -2\rho N_\kappa & \rho I \end{bmatrix},$$

we observe that (3.17a) can be written as  
(3.17b)

$$\begin{aligned} \text{GFK} \begin{bmatrix} \gamma_D u^t \\ \gamma_N^1 u^t \end{bmatrix} &:= \begin{bmatrix} \frac{1}{2}I + K_2 & -\rho^{-1}S_2 \\ \rho N_2 & \frac{1}{2}I - K_2^\top \end{bmatrix} \begin{bmatrix} \gamma_D u^t \\ \gamma_N^1 u^t \end{bmatrix} + R \text{CFK} \begin{bmatrix} \gamma_D u^t \\ \gamma_N^1 u^t \end{bmatrix} \\ &= R \begin{bmatrix} \gamma_D u^{\text{inc}} \\ \gamma_N u^{\text{inc}} \end{bmatrix}. \end{aligned}$$

We will refer to this formulation as *regularized combined field integral equations* (CFIER).

Another possible formulation of transmission problems (2.1)–(2.3) takes on the form of *single* integral equations [21]. The main idea is to look for the field  $u^2$  as a single layer potential, that is,

$$u^2(\mathbf{z}) = -2[SL_2\mu](\mathbf{z}), \quad \mathbf{z} \in D_2,$$

where  $\mu$  is an *aphysical* density defined on  $\Gamma$ . The transmission boundary conditions (2.3) and the trace relations (3.1) imply first

$$\gamma_D u^t = -2S_2\mu, \quad \gamma_N^1 u^t = -\rho(I + 2K_2^\top)\mu,$$

and second, from (3.14),

$$u^1(\mathbf{z}) = \rho SL_1[(I + 2K_2^\top)\mu](\mathbf{z}) - 2DL_1[S_2\mu](\mathbf{z}), \quad \mathbf{z} \in D_1.$$

Using these representations of the fields  $u^1$  and  $u^2$ , the Neumann and Dirichlet traces of  $u^1$  and  $u^2$  on  $\Gamma$  are used in a Burton-Miller type combination of the form  $(\gamma_N^1 u^1 - i\eta\gamma_D^1 u^1) - (\rho\gamma_N^2 u^2 - i\eta\gamma_D^2 u^2) = -\gamma_N u^{\text{inc}} + i\eta\gamma_D u^{\text{inc}}$ , cf., [10] to lead to the following boundary integral equation

(3.18)

$$\text{SIE } \mu := -\frac{1 + \rho}{2}\mu + \mathbf{K}\mu - i\eta\mathbf{S}\mu = \gamma_N u^{\text{inc}} - i\eta\gamma_D u^{\text{inc}}, \quad 0 \neq \eta \in \mathbb{R},$$

where

$$\mathbf{K} = -K_2^\top(\rho I - 2K_2^\top) - \rho K_1^\top(I + 2K_2^\top) + 2(N_1 - N_2)S_2$$

and

$$\mathbf{S} = -\rho S_1(I + 2K_2^\top) - (I - 2K_1)S_2.$$

We refer in what follows to equation (3.18) as SCFIE. The coupling parameter  $\eta$  in equations (3.18) is typically taken to be equal to  $k_1$ .

**4. Existence and uniqueness for the boundary integral formulations CFIEFK (3.15), CFIESK (3.16), CFIER (3.17) and SCFIE (3.18).** In this section, we state the well-posedness of the boundary integral formulations on Lipschitz curves presented in the previous section. Let us point out that, with very minor and direct modifications, the proofs of the main results of this section can be adapted to the case of Lipschitz domains in  $3D$ . Hence, these formulations are well-posed as well, and the associated integral operators satisfy the same properties in the Sobolev frame. Since, in this paper, we have focused our attention on bidimensional domains, we have preferred to work only on Lipschitz curves for the sake of simplicity.

One of the basic tools we will use in the analysis developed in this section consists of comparing the boundary operators for the Helmholtz equation with those for Laplace operator,  $S_0$ ,  $K_0$ ,  $K_0^\top$  and  $N_0$  which are defined as the corresponding boundary Helmholtz operators in Section 3 using

$$G_0(\mathbf{x}) = -\frac{1}{2\pi} \log |\mathbf{x}|,$$

the fundamental solution of the Laplace operator, instead.

**4.1. Sobolev spaces and functional properties of boundary operators.** For any domain  $D \subset \mathbb{R}^2$  with bounded Lipschitz boundary  $\Gamma$ , we denote by  $H^s(D)$  the classical Sobolev space of order  $s$  on  $D$  (see, for example, the excellent textbooks [1, Chapter 2] or [30, Chapter 3]). We consider in addition the Sobolev spaces defined on the boundary  $\Gamma$ ,  $H^s(\Gamma)$ , which are well defined for any  $s \in [-1, 1]$ . It is well known that, for smoother  $\Gamma$ , the range for these  $s$  can be widened but we do not make use of these spaces in this section. We recall that, for any  $s > t$ ,  $H^s(\Sigma) \subset H^t(\Sigma)$ ,  $\Sigma \in \{D_1, D_2, \Gamma\}$  with continuous and compact

embedding. Moreover,  $(H^t(\Gamma))' = H^{-t}(\Gamma)$  when the inner product of  $H^0(\Gamma) = L^2(\Gamma)$  is used as the duality product.

It is well known that  $\gamma_D^j : H^{s+1/2}(D_j) \rightarrow H^s(\Gamma)$  is continuous for  $s \in (0, 1)$ , and if

$$H_\Delta^s(D_j) := \{U \in H^s(D_j) : \Delta U \in L^2(D_j)\},$$

endowed with its natural norm, then  $\gamma_N : H_\Delta^s(D_j) \rightarrow H^{s-3/2}(\Gamma)$  is continuous for  $s \in (1/2, 3/2)$ .

The space  $H^1(\Gamma)$ , and its dual  $H^{-1}(\Gamma)$ , are then the limit cases from several different perspectives. Let  $\nabla_\Gamma$  be the tangential derivative defined as

$$\nabla_\Gamma(U|_\Gamma) = \partial_s(U|_\Gamma) \boldsymbol{\tau}$$

where  $\boldsymbol{\tau}$  denotes (one of) the unit tangent vector fields to  $\Gamma$ , and  $\partial_s$  the tangential derivative with respect to  $\boldsymbol{\tau}$ . It is known that an integral expression for the (or an equivalent) inner product in  $H^1(\Gamma)$  is given by

$$(4.1) \quad \begin{aligned} (u, v)_{H^1(\Gamma)} &:= \int_\Gamma \nabla_\Gamma u \cdot \overline{\nabla_\Gamma v} + \int_\Gamma u \bar{v} \\ &= \langle \boldsymbol{\Lambda} u, \overline{\boldsymbol{\Lambda} v} \rangle, \quad \boldsymbol{\Lambda} u := \nabla_\Gamma u + u \mathbf{n} \end{aligned}$$

We commit here a slight abuse of notation, and denote with the same symbol  $\langle \cdot, \cdot \rangle$  the non-complex integral inner product in  $(L^2(\Gamma))^2$ .

**Theorem 4.1.** *Let  $D_2$  be a bounded domain, with Lipschitz boundary  $\Gamma$ , and set  $D_1 := \mathbb{R}^2 \setminus \overline{D_2}$ . Then, if  $\chi \in C^\infty(\mathbb{R}^2)$  with compact support,*

- $SL_k : H^s(\Gamma) \rightarrow H^{s+3/2}(D_2), \chi SL_k : H^s(\Gamma) \rightarrow H^{s+3/2}(D_1),$
- $DL_k : H^{s+1}(\Gamma) \rightarrow H^{s+3/2}(D_2), \chi DL_k : H^{s+1}(\Gamma) \rightarrow H^{s+3/2}(D_1)$

are continuous for  $s \in [-1, 0]$ . Moreover,

- $S_k : H^s(\Gamma) \rightarrow H^{s+1}(\Gamma),$
- $K_k : H^{s+1}(\Gamma) \rightarrow H^{s+1}(\Gamma),$
- $K_k^\top : H^s(\Gamma) \rightarrow H^s(\Gamma),$
- $N_k : H^{s+1}(\Gamma) \rightarrow H^s(\Gamma),$

are continuous for  $s \in [-1, 0]$ .

A proof for the intermediate values  $s \in (-1, 0)$  can be found in [12, Theorem 1] (see also [30, Theorem 6.12]). The proofs for  $k = 0$ , the Laplace operator, and  $s = -1, 0$  can be found in [37] (see also the comments following [30, Theorem 6.12]). For  $k \neq 0$ , the argument follows by showing that the difference between the corresponding Laplace and Helmholtz boundary operators are smooth enough. We refer to the discussion [30, end of Chapter 6] or that following [12, Theorem 1] and the references therein. For the sake of completeness, we next give a proof of this result. This result will actually be used to prove the well posedness of the different formulations considered in this paper.

First we will need this technical lemma which will be proven for the sake of completeness.

**Lemma 4.2.** *The integral operators*

$$\mathbf{\Lambda}(K_{k_1} - K_{k_2}), \quad N_{k_1} - N_{k_2}$$

*have weakly (integrable) singular kernels.*

*Proof.* Without loss of generality, we can assume in this proof that  $k_2 = 0$ . The kernel of  $\mathbf{\Lambda}(K_{k_1} - K_0)$  is then given (almost everywhere) by

$$- \mathbf{n}(\mathbf{x}) [(\nabla(G_{k_1} - G_0)(\mathbf{x} - \mathbf{y})) \cdot \mathbf{n}(\mathbf{y})] - \boldsymbol{\tau}(\mathbf{x}) [\boldsymbol{\tau}^\top(\mathbf{x}) (\nabla^2(G_{k_1} - G_0)(\mathbf{x} - \mathbf{y})) \mathbf{n}(\mathbf{y})], \quad \mathbf{x}, \mathbf{y} \in \Gamma.$$

( $\nabla^2 G$  above denotes the Hessian matrix of  $G$ ), whereas

$$- \mathbf{n}^\top(\mathbf{x}) (\nabla^2(G_{k_1} - G_0)(\mathbf{x} - \mathbf{y})) \mathbf{n}(\mathbf{y})$$

is the kernel of  $N_{k_1} - N_0$ .

Then it suffices to show that, for any  $R > 0$ , there exists  $C_R > 0$  such that

$$(4.2) \quad |\nabla(G_{k_1} - G_0)(\mathbf{x})| + \|\nabla^2(G_{k_1} - G_0)(\mathbf{x})\| \leq C_R(1 + \log |\mathbf{x}|),$$

for  $0 < |\mathbf{x}| < R$ , where  $\|\cdot\|$  above is any matrix norm.

The proof of this bound relies on analytical properties of the Hankel functions, namely, the behavior at zero and appropriate decompositions of these functions. We point out that a deeper analysis on this topic will

be carried out in Section 5, so that we limit ourselves to the exposition of the properties we are going to use.

With the identity  $(H_0^{(1)})'(z) = -H_1^{(1)}(z)$ , we can first obtain

$$(4.3) \quad \nabla(G_{k_1} - G_0)(\mathbf{x}) = \left( -\frac{i}{4}H_1^{(1)}(k_1|\mathbf{x}|)k_1|\mathbf{x}| + \frac{1}{2\pi} \right) \frac{\mathbf{x}^\top}{|\mathbf{x}|^2}$$

(we follow the convention of writing the gradient as a row vector). Note now that

$$\frac{i}{4}zH_1^{(1)}(z) = -\frac{1}{2\pi}J_1(z)z \log z + \frac{1}{2\pi} + d_1(z)z^2,$$

where  $J_1$  is the Bessel function which is known to be smooth, with  $J_1(0) = 0$ ,  $J_1'(0) = 1/2$  and  $d_1$  being smooth as well. From this decomposition, we deduce easily that  $\nabla(G_{k_1} - G_0)$  satisfies (4.2).

On the other hand, using that

$$\left( zH_1^{(1)}(z) \right)' = zH_0^{(1)}(z).$$

we can easily show that

$$\begin{aligned} \nabla^2(G_{k_1} - G_0)(\mathbf{x}) &= -\frac{ik_1^2}{4}H_0^{(1)}(k_1|\mathbf{x}|)\frac{1}{|\mathbf{x}|^2}\mathbf{x}\mathbf{x}^\top \\ &+ \left( \frac{i}{4}H_1^{(1)}(k_1|\mathbf{x}|)k_1|\mathbf{x}| - \frac{1}{2\pi} \right) \left( \frac{2}{|\mathbf{x}|^4}\mathbf{x}\mathbf{x}^\top - \frac{1}{|\mathbf{x}|^2}I \right), \end{aligned}$$

where  $I$  is  $2 \times 2$  identity matrix.

Since, in addition,

$$\frac{i}{4}H_0^{(1)}(z) = -\frac{1}{2\pi}J_0(z) \log z + c_0(z)$$

where  $J_0$  (the Bessel function) and  $c_0$  are smooth, a simple inspection shows that the entries of the Hessian matrix can be bounded by  $C \log(|\mathbf{x}|)$  on any punctured ball around  $\mathbf{0}$  with appropriate constant  $C$  (which depends obviously on  $k_1$  and on the diameter of the domain). □

**Theorem 4.3.** *Let  $k_1 \neq k_2$ . Then*

- $S_{k_1} - S_{k_2} : H^{-1}(\Gamma) \rightarrow H^1(\Gamma)$ ,
- $K_{k_1} - K_{k_2} : H^0(\Gamma) \rightarrow H^1(\Gamma)$ ,
- $K_{k_1}^\top - K_{k_2}^\top : H^{-1}(\Gamma) \rightarrow H^0(\Gamma)$ ,
- $N_{k_1} - N_{k_2} : H^0(\Gamma) \rightarrow H^0(\Gamma)$ .

*are continuous and compact.*

*Proof.* It is a well-known consequence of the Lax theorem (see [24, Theorem 4.12]) that integral operators with weakly singular kernels define compact operators in  $L^2$ . From this fact, and Lemma 4.2, we see that

$$N_{k_1} - N_{k_2} : H^0(\Gamma) \longrightarrow H^0(\Gamma)$$

is compact.

Similarly,

$$\mathbf{\Lambda}(K_{k_1} - K_{k_2}) : H^0(\Gamma) \longrightarrow [H^0(\Gamma)]^2$$

is also compact (again from Lemma 4.2).

Consider now a weakly convergent sequence  $(u_n)_n$ . Then  $(\mathbf{\Lambda}(K_{k_1} - K_{k_2})u_n)_n$  converges strongly, by the compactness of the operator, in  $[H^0(\Gamma)]^2$  and, because identity (4.1) holds,  $((K_{k_1} - K_{k_2})u_n)_n$  is strongly convergent in  $H^1(\Gamma)$ . In other words,  $K_{k_1} - K_{k_2} : H^0(\Gamma) \rightarrow H^1(\Gamma)$  is compact as well.

A duality argument now proves the result for  $K_{k_1}^\top - K_{k_2}^\top$ .

Finally, assume, without loss of generality, that  $k_1$  is taken so that  $N_{k_1} : H^0(\Gamma) \rightarrow H^{-1}(\Gamma)$  is invertible. (It suffices to take as  $k_1$  a pure imaginary number). Then

$$\begin{aligned} S_{k_1} - S_{k_2} &= N_{k_1}^{-1} [N_{k_1} S_{k_1} - N_{k_2} S_{k_2}] + N_{k_1}^{-1} (N_{k_2} - N_{k_1}) S_{k_2} \\ (4.4) \quad &= N_{k_1}^{-1} [(K_{k_1}^\top)^2 - (K_{k_2}^\top)^2] + N_{k_1}^{-1} (N_{k_2} - N_{k_1}) S_{k_2} \\ &= N_{k_1}^{-1} [K_{k_1}^\top - K_{k_2}^\top] K_{k_2}^\top + N_{k_1}^{-1} K_{k_1}^\top [K_{k_1}^\top - K_{k_2}^\top] \\ &\quad + N_{k_1}^{-1} (N_{k_2} - N_{k_1}) S_{k_2}, \end{aligned}$$

where we have applied the second identity in equation (3.9). In view of identity (4.4) and the mapping properties of the operators involved, we

conclude that  $S_{k_2} - S_{k_1} : H^{-1}(\Gamma) \rightarrow H^1(\Gamma)$  is continuous and compact. The proof is now finished.  $\square$

The last ingredient in our proof is this result due to Escauriaza, Fabes and Verchota [14]. In this result,  $K_0$  and  $K_0^\top$  are the double and adjoint double layer operators for the Laplace equation (which obviously corresponds to  $k = 0$ ).

**Theorem 4.4.** *For any Lipschitz curve and  $\lambda \notin (-1/2, 1/2]$ , the mappings*

$$\lambda I + K_0 : H^s(\Gamma) \longrightarrow H^s(\Gamma), \quad \lambda I + K_0^\top : H^{-s}(\Gamma) \longrightarrow H^{-s}(\Gamma)$$

are invertible for  $s \in [0, 1]$ . Moreover,

$$\frac{1}{2}I + K_0 : H^s(\Gamma) \longrightarrow H^s(\Gamma), \quad \frac{1}{2}I + K_0^\top : H^{-s}(\Gamma) \longrightarrow H^{-s}(\Gamma)$$

are Fredholm of index 0.

*Proof.* In [37, Theorems 3.1, 3.3], it is proven that  $-\frac{1}{2}I + K_0 : H^s(\Gamma) \rightarrow H^s(\Gamma)$  is invertible for  $s = 0, 1$ . (Note that in this paper  $\frac{1}{2\pi} \log |\mathbf{x}| = -G_0(\mathbf{x})$  is taken as a fundamental solution.) By interpolation of Sobolev spaces and a transposition argument, we can prove the result for  $\lambda = -1/2$ .

In [14, Theorem 2], the result is proven for  $|\lambda| > 1/2$  and  $s = 0$ . To extend the result for the remaining  $s$  we can adapt the argument outlined in [37]. Suppose that  $S_0 : H^0(\Gamma) \rightarrow H^1(\Gamma)$  is invertible. Then,  $S_0(\lambda I + K_0)S_0^{-1} : H^1(\Gamma) \rightarrow H^1(\Gamma)$  is invertible as well. But Calderon identities (3.9) imply

$$(4.5) \quad S_0(\lambda I + K_0)S_0^{-1} = (\lambda I + K_0^\top)S_0S_0^{-1} = (\lambda I + K_0^\top)$$

from which we conclude the invertibility, for  $\lambda \notin (-1/2, 1/2]$ , of  $\lambda I + K_0^\top : H^s(\Gamma) \rightarrow H^s(\Gamma)$  first for  $s = -1$  and next, by interpolation, for  $s \in [-1, 0]$ . Again, by transposition, we can show that  $\lambda I + K_0 : H^s(\Gamma) \rightarrow H^s(\Gamma)$  is invertible for  $s \in [0, 1]$ . This argument breaks down when  $S_0$  is not invertible, that is, when the logarithmic capacity of the curve  $\Gamma$  is 1. For this case, we consider

$$\tilde{S}_0\varphi := S_0\varphi + \int_{\Gamma} \varphi.$$

It can be shown that  $\tilde{S}_0 : H^s(\Gamma) \rightarrow H^{s+1}(\Gamma)$  is continuous and invertible for  $s \in [-1, 0]$  (see [30, Chapter 8]). Moreover, since

$$\int_{\Gamma} K_0 \varphi = K_0^\top \left( \int_{\Gamma} \varphi \right),$$

we still have  $K_0 \tilde{S}_0 = \tilde{S}_0 K_0^\top$ , which makes it possible to extend the argument in (4.5), with  $\tilde{S}_0$  instead, to this case as well.

Finally, in [37, Theorem 4.2], it is proven that  $\frac{1}{2}I + K_0^\top : L_0^2(\Gamma) \rightarrow L_0^2(\Gamma)$  is invertible where  $L_0^2(\Gamma)$  is the subspace of functions in  $L^2(\Gamma) = H^0(\Gamma)$  with zero mean. Then  $\dim N(\frac{1}{2}I + K_0^\top) = \text{codim } R(\frac{1}{2}I + K_0^\top) = 1$ , which in particular, implies that  $\frac{1}{2}I + K_0^\top : H^0(\Gamma) \rightarrow H^0(\Gamma)$  is Fredholm of index zero and, by transposition, so is  $\frac{1}{2}I + K_0 : H^0(\Gamma) \rightarrow H^0(\Gamma)$ . The same argument as before extends this result to  $H^s(\Gamma)$ .  $\square$

Observe that, in the proof of this last result, we have assumed that  $\Gamma$  is simply connected. Otherwise,  $\dim N(\frac{1}{2}I + K_0^\top) = \text{codim } R(\frac{1}{2}I + K_0^\top)$  equals the number of simply connected components, and the argument is still valid with this very minor modification.

**4.2. Well-posedness of the boundary integral equation formulations CFIEFK (3.15), CFIER (3.17) and SCFIE (3.18).**

In this section, we state and prove the well posedness of the integral equation formulations for transmission problems. For Costabel-Stephan CFIEFK (3.15) and Kress-Roach CFIESK (3.16) formulations, the stability has already been proved, but only in the space  $H^{1/2}(\Gamma) \times H^{-1/2}(\Gamma)$  [13, 36]. We will, however, extend these results to a wider range of Sobolev spaces. To this end, we make use of the skew-symmetric bilinear form

$$\langle\langle (f, \varphi), (g, \psi) \rangle\rangle := \int_{\Gamma} f\psi - \int_{\Gamma} g\varphi, \quad (f, \varphi), (g, \psi) \in H^{1/2}(\Gamma) \times H^{-1/2}(\Gamma)$$

which gives a non-usual representation, but more convenient for our purposes, of the duality product between  $H^{1/2}(\Gamma) \times H^{-1/2}(\Gamma)$  and itself. Obviously, the integrals above must be understood in a weak sense if  $\varphi$  and  $\psi$  are not sufficiently smooth.

We point out that, if

$$A : H^{1/2}(\Gamma) \times H^{-1/2}(\Gamma) \longrightarrow H^{1/2}(\Gamma) \times H^{-1/2}(\Gamma),$$

with  $A = (A_{ij})_{i,j=1}^2$ , then the transpose operator

$$\langle A^t(f, \varphi), (g, \psi) \rangle := \langle (f, \varphi), A(g, \psi) \rangle,$$

for all  $(f, \varphi), (g, \psi) \in H^{1/2}(\Gamma) \times H^{-1/2}(\Gamma)$ ,

is given by

$$(4.6) \quad A^t = \begin{bmatrix} & 1 \\ -1 & \end{bmatrix} A^\top \begin{bmatrix} & 1 \\ -1 & \end{bmatrix} = \begin{bmatrix} A_{22}^\top & -A_{12}^\top \\ -A_{21}^\top & A_{11}^\top \end{bmatrix}.$$

Here,  $A_{ij}^\top$  is simply the adjoint of  $A_{ij}$  in the bilinear form defined by the integral product in  $\Gamma$ . Observe that the familiar identity  $(AB)^t = B^t A^t$  still holds.

**Theorem 4.5.** *The following operators*

$$\text{CSK} : H^s(\Gamma) \times H^{s-1}(\Gamma) \longrightarrow H^s(\Gamma) \times H^{s-1}(\Gamma),$$

$$\text{CFK} : H^s(\Gamma) \times H^{s-1}(\Gamma) \longrightarrow H^s(\Gamma) \times H^{s-1}(\Gamma)$$

are invertible with continuous inverses for all  $s \in [0, 1]$ .

*Proof.* Assume  $\rho \neq 1$ . Note that, from (3.16),

$$\begin{aligned} \text{CSK} = & \frac{\rho - 1}{\rho} \underbrace{\begin{bmatrix} \frac{\rho+1}{2(\rho-1)}I + K_0 & \\ & \frac{\rho+1}{2(\rho-1)}I + K_0^\top \end{bmatrix}}_{\text{CSK}_0} \\ & + \underbrace{\begin{bmatrix} K_2 - K_0 - \rho^{-1}(K_1 - K_0) & \rho^{-1}(S_1 - S_2) \\ -(N_1 - N_2) & K_1^\top - K_0^\top - \rho^{-1}(K_2^\top - K_0^\top) \end{bmatrix}}_{L_1} \end{aligned}$$

(here  $K_0$  and  $K_0^\top$  denote the double layer and adjoint double layer operators, respectively, for the Laplace equation). Clearly,

$$\frac{\rho + 1}{2(\rho - 1)} \in \mathbb{R} \setminus [-1/2, 1/2].$$

By Theorem 4.3,  $L_1 : H^0(\Gamma) \times H^{-1}(\Gamma) \rightarrow H^1(\Gamma) \times H^0(\Gamma)$  is continuous and compact. On the other hand,  $\text{CSK}_0 : H^s(\Gamma) \times H^{s-1}(\Gamma) \rightarrow H^s(\Gamma) \times H^{s-1}(\Gamma)$  is invertible by Theorem 4.4. Therefore, CSK is Fredholm of index zero with kernel in  $H^1(\Gamma) \times H^0(\Gamma)$ . For  $\rho = 1$ , the proof is even simpler since now Theorem 4.3 shows that CSK is

a compact perturbation of the identity in  $H^s(\Gamma) \times H^{s-1}(\Gamma)$ , and the same argument can be applied to prove that the kernel is contained in  $H^1(\Gamma) \times H^0(\Gamma)$  as well.

Injectivity can be shown using Green identities and the uniqueness of the transmission problem, cf., [13]. We emphasize that the regularity of the kernel of CSK is crucial to making the arguments in [13] valid.

For the second operator, we first note that

$$\text{CFK} = \underbrace{\begin{bmatrix} -2K_0 & \frac{\rho+1}{\rho}S_0 \\ -(1+\rho)N_0 & 2K_0^\top \end{bmatrix}}_{\text{CFK}_0} + L_2,$$

where  $L_2 : H^0(\Gamma) \times H^{-1}(\Gamma) \rightarrow H^1(\Gamma) \times H^0(\Gamma)$  is again compact. Calderón identities in (3.9) yield that (see also (4.6))

$$\begin{aligned} \text{CFK}_0^t \text{CFK}_0 &= \begin{bmatrix} 2K_0 & -\frac{\rho+1}{\rho}S_0 \\ (1+\rho)N_0 & -2K_0^\top \end{bmatrix} \begin{bmatrix} -2K_0 & \frac{\rho+1}{\rho}S_0 \\ -(1+\rho)N_0 & 2K_0^\top \end{bmatrix} \\ &= \begin{bmatrix} -4K_0^2 + \frac{(\rho+1)^2}{\rho}S_0N_0 & \frac{2(\rho+1)}{\rho}(K_0S_0 - S_0K_0^\top) \\ -2(\rho+1)(N_0K_0 - K_0^\top N_0) & -4(K_0^\top)^2 + \frac{(\rho+1)^2}{\rho}N_0S_0 \end{bmatrix} \\ &= \frac{(\rho-1)^2}{\rho} \begin{bmatrix} -\frac{(\rho+1)^2}{4(\rho-1)^2}I + K_0^2 & \\ & -\frac{(\rho+1)^2}{4(\rho-1)^2}I + (K_0^\top)^2 \end{bmatrix} \\ &= \frac{(\rho-1)^2}{\rho} \begin{bmatrix} (-\beta I + K_0)(\beta I + K_0) & \\ & (-\beta I + K_0^\top)(\beta I + K_0^\top) \end{bmatrix}, \end{aligned}$$

$$\beta := \frac{\rho+1}{2\rho-2}.$$

Theorem 4.4, observe that  $|\beta| > 1/2$ , implies that this mapping is invertible, and therefore, so is  $\text{CFK}_0$ . We then conclude that

$$\text{CFK} : H^s(\Gamma) \times H^{s-1}(\Gamma) \longrightarrow H^s(\Gamma) \times H^{s-1}(\Gamma)$$

is Fredholm of index zero. If  $\rho = 1$ ,

$$\text{CFK}_0^t \text{CFK}_0 = - \begin{bmatrix} I & \\ & I \end{bmatrix},$$

which makes the argument valid. Injectivity, which implies invertibility by the Fredholm alternative, follows using classical arguments, cf., [36]. □

We would like to point out that the original proof for invertibility of CFK is based, in a nutshell, on showing that its principal part is coercive (strongly elliptic) in the space  $H^{1/2}(\Gamma) \times H^{-1/2}(\Gamma)$ , cf., [13, Section 5].

**Theorem 4.6.** *Assume that the wavenumber  $\kappa$  in (3.17) has a positive imaginary part. Then the operators*

$$\text{GFK} : H^s(\Gamma) \times H^{s-1}(\Gamma) \longrightarrow H^s(\Gamma) \times H^{s-1}(\Gamma)$$

*are invertible with continuous inverses in the spaces  $H^s(\Gamma) \times H^{s-1}(\Gamma)$  for all  $s \in [0, 1]$ .*

*Proof.* We first prove that GFK is a compact perturbation of an invertible operator. Beginning with (3.17b), and proceeding as above, we derive

$$\begin{aligned} \text{GFK} &= \underbrace{\begin{bmatrix} \frac{1}{2}I + K_0 & -\rho^{-1}S_0 \\ \rho N_0 & \frac{1}{2}I - K_0^\top \end{bmatrix}}_{L_0} \\ &\quad + \frac{1}{\rho + 1} \underbrace{\begin{bmatrix} I & 2S_0 \\ -2\rho N_0 & \rho I \end{bmatrix}}_{R_0} \text{CFK}_0 + L_3 \\ &=: \text{GFK}_0 + L_3, \end{aligned}$$

with  $L_3 : H^0(\Gamma) \times H^{-1}(\Gamma) \rightarrow H^1(\Gamma) \times H^0(\Gamma)$  compact. Straightforward calculations show that  $L_0^t L_0 = 0$ ,

$$\begin{aligned} &\text{CFK}_0^t R_0^t R_0 \text{CFK}_0 = \\ &\frac{4(\rho - 1)^2}{(\rho + 1)^2} \begin{bmatrix} K_0^2 \left(-\frac{\rho+1}{2(\rho-1)} I + K_0\right) \left(\frac{\rho+1}{2(\rho-1)} I + K_0\right) & \\ & (K_0^\top)^2 \left(-\frac{\rho+1}{2(\rho-1)} I + K_0^\top\right) \left(\frac{\rho+1}{2(\rho-1)} I + K_0^\top\right) \end{bmatrix} \end{aligned}$$

$$\begin{aligned} &L_0^t R_0 \text{CFK}_0 + \text{CFK}_0^t R_0^t L_0 \\ &= -\frac{2(\rho - 1)}{\rho + 1} \begin{bmatrix} (-I + 2K_0^2) \left(\frac{\rho+1}{2(\rho-1)} I + K_0\right) & \\ & (-I + 2(K_0^\top)^2) \left(\frac{\rho+1}{2(\rho-1)} I + (K_0^\top)\right) \end{bmatrix}. \end{aligned}$$

Therefore,

$$(4.7) \quad \text{GFK}_0^t \text{GFK}_0 = \begin{bmatrix} A_1 & \\ & A_1^\top \end{bmatrix},$$

where

$$A_1 := \frac{4(\rho - 1)^2}{(\rho + 1)^2} \left( K_0 + \frac{\rho + 1}{2(\rho - 1)} I \right) \left( K_0^3 - \frac{3(\rho + 1)}{2(\rho - 1)} K_0^2 + \frac{\rho + 1}{2(\rho - 1)} I \right).$$

Note that

$$A_1 = \frac{4(\rho - 1)^2}{(\rho + 1)^2} \left( \frac{\rho + 1}{2(\rho - 1)} I + K_0 \right) \begin{aligned} &(-\lambda_1(\rho)I + K_0) \\ &(-\lambda_2(\rho)I + K_0)(-\lambda_3(\rho)I + K_0) \end{aligned}$$

where  $\lambda_j(\rho)$  are the roots of

$$p_\rho(x) = x^3 - \frac{3(\rho + 1)}{2(\rho - 1)} x^2 + \frac{\rho + 1}{2(\rho - 1)},$$

which can be shown to be all real and lying outside of  $[-1/2, 1/2]$  for any  $\rho \in (0, \infty) \setminus \{1\}$ , cf., Lemma 4.7 below. Theorem 4.4 implies the invertibility of  $A_1$  and therefore of  $\text{GFK}_0$ .

For  $\rho = 1$ , the proof clearly breaks down, but it can be studied separately and the deduction obtained that (4.7) still holds with

$$A_1 = 1 - 3K_0^2 = -3 \left( \frac{1}{\sqrt{3}} I + K_0 \right) \left( -\frac{1}{\sqrt{3}} I + K_0 \right),$$

which again is invertible.

In short, we have shown that  $\text{GFK} : H^s(\Gamma) \times H^{s-1}(\Gamma) \rightarrow H^s(\Gamma) \times H^{s-1}(\Gamma)$ , for  $s \in [0, 1]$ , is Fredholm of index zero. To prove that it is invertible we will consider the adjoint operator given by (see (3.17b))

$$\begin{aligned} \text{GFK}^t &= \begin{bmatrix} \frac{1}{2}I - K_2 & \rho^{-1}S_2 \\ -\rho N_2 & \frac{1}{2}I + K_2^\top \end{bmatrix} \\ &+ \begin{bmatrix} (K_1 + K_2) & -(\rho^{-1}S_2 + S_1) \\ N_1 + \rho N_2 & -(K_1^\top + K_2^\top) \end{bmatrix} \frac{1}{1 + \rho} \begin{bmatrix} \rho I & -2S_\kappa \\ 2\rho N_\kappa & I \end{bmatrix}. \end{aligned}$$

We note that the operator  $\text{GFK}^t$  is exactly the one corresponding to the GCSIE formulations [4, 5]. Clearly,

$$\text{GFK}^t = \text{GFK}_0^t + \text{L}_3^t,$$

where  $\text{GFK}_0^t : H^s(\Gamma) \times H^{s-1}(\Gamma) \rightarrow H^s(\Gamma) \times H^{s-1}(\Gamma)$  is invertible for  $s \in [0, 1]$  and  $\text{L}_3^t : H^0(\Gamma) \times H^{-1}(\Gamma) \rightarrow H^1(\Gamma) \times H^0(\Gamma)$  is compact. Then,

the null space of this operator is contained in  $H^1(\Gamma) \times H^0(\Gamma)$ . We can then follow the arguments in [5] and conclude  $\text{GFK}^t$  is injective (the arguments are still valid for Lipschitz domains once we ensure that the elements of the null space are smooth enough), and therefore, from the Fredholm alternative, invertible from where one derives the invertibility of our operator  $\text{GFK}$ .  $\square$

**Lemma 4.7.** *For any positive  $\rho \neq 1$ , the roots of the polynomial,*

$$x^3 - \frac{3(\rho + 1)}{2(\rho - 1)}x^2 + \frac{\rho + 1}{2(\rho - 1)},$$

*are all real and lie outside the interval  $[-1/2, 1/2]$ .*

*Proof.* We can reduce the problem to study of the polynomial

$$q_\beta(x) = x^3 - 3\beta x^2 + \beta$$

for  $\beta = (\rho + 1)/[2(\rho - 1)] \in \mathbb{R} \setminus [-1/2, 1/2]$ .

Assume  $\beta > 1/2$ . Then  $q_\beta(\pm\frac{1}{2}) = \pm\frac{1}{8} + \frac{\beta}{4}$ , that is,  $q_\beta(\pm 1/2) > 0$ . Also,  $q_\beta(2\beta) = 4\beta(\frac{1}{4} - \beta^2) < 0$ , and thus,  $q_\beta$  has a zero between  $1/2$  and  $2\beta$ . Furthermore, since  $\lim_{x \rightarrow \mp\infty} q_\beta(x) = \mp\infty$ , it follows that  $q_\beta$  must have one (real) zero in  $(-\infty, -1/2)$ , and another zero in  $(2\beta, \infty)$ . Hence, we have shown that the three roots of the polynomial are real and lie outside the interval  $[-1/2, 1/2]$ .

For  $\beta < -1/2$ , one can show, similarly, that  $q_\beta$ , has three real roots, two of them smaller than  $-1/2$ , and the other one larger than  $1/2$ .  $\square$

We end this section with the study of the SCFIE formulation (3.18) which again turns out to be stable, although in weaker norms.

**Theorem 4.8.** *The operator  $\text{SIE} : H^s(\Gamma) \rightarrow H^s(\Gamma)$  associated to the formulation SCFIE (3.18) is invertible for any  $s \in [-1, 0]$ .*

*Proof.* It can be easily seen that, if  $\rho \neq 1$ , we have

$$\begin{aligned} \text{SIE} &= 2(1 - \rho) \left( -\frac{1 + \rho}{4(1 - \rho)} I - \frac{\rho}{1 - \rho} K_0^\top + \left( K_0^\top \right)^2 \right) + L_4 \\ &= 2(1 - \rho) \left( \frac{1}{2} I + K_0^\top \right) \left( -\frac{\rho + 1}{2(\rho - 1)} I + K_0^\top \right) + L_4, \end{aligned}$$

where  $L_4 : H^{-1} \rightarrow H^0$  can be checked for compactness. We have that the operator  $\frac{1}{2}I + K_0^\top$  is Fredholm of index zero (cf., Theorem 4.4) while the operator  $-(\rho + 1)/[2(\rho - 1)]sI + K_0^\top$  is invertible, and thus the main part of the SIE operator is Fredholm of index zero as well which is enough for our purposes. The Fredholm alternative now implies the invertibility of SIE. (We refer to the seminal paper [21] for a proof of the injectivity). The case  $\rho = 1$  can be treated similarly.  $\square$

**5. High-order Nyström methods for the discretization of the formulations CFIEFK (3.15), CFIESK (3.16), CFIER (3.17) and SCFIE (3.18).** In this section, we present Nyström discretizations of formulations CFIEFK (3.15), CFIESK (3.16), CFIER (3.17b) and SCFIE (3.18) where were presented in the previous section. The discretizations of some of these formulations, for smooth curves, have been already analyzed in [7]. The key component for polygonal domains is to use sigmoidal-graded meshes that accumulate points polynomially at corners and to reformulate the aforementioned systems of integral equations in terms of *more regular densities* and weighted versions of the boundary integral operators of Helmholtz equations.

**5.1. Weighted boundary integral operators for the Helmholtz equation.** We assume that the domain  $D$  has corners at  $\mathbf{x}_1, \mathbf{x}_2, \dots, \mathbf{x}_P$  whose apertures measured inside  $D$  are respectively  $\theta_1, \theta_2, \dots, \theta_P$ , and that  $\Gamma \setminus \{\mathbf{x}_1, \mathbf{x}_2, \dots, \mathbf{x}_P\}$  is piecewise analytic. Let  $(x_1(t), x_2(t))$  be a  $2\pi$  periodic parametrization of  $\Gamma$  so that each of the curved segments  $[\mathbf{x}_j, \mathbf{x}_{j+1}]$  is mapped by  $(x_1(t), x_2(t))$  with  $t \in [T_j, T_{j+1}]$ . We assume that  $x_1(t), x_2(t)$  are continuous and that on each interval  $[T_j, T_{j+1}]$  are smooth with  $(x_1'(t))^2 + (x_2'(t))^2 > 0$  (the one-sided derivatives are taken for  $t = T_j, T_{j+1}$ ). Consider the sigmoid transform introduced by Kress in [22]

(5.1)

$$w(s) = \frac{T_{j+1}[v(s)]^p + T_j[1 - v(s)]^p}{[v(s)]^p + [1 - v(s)]^p}, \quad T_j \leq s \leq T_{j+1}, \quad 1 \leq j \leq P$$

$$v(s) = \left(\frac{1}{p} - \frac{1}{2}\right) \left(\frac{T_j + T_{j+1} - 2s}{T_{j+1} - T_j}\right)^3 + \frac{1}{p} \frac{2s - T_j - T_{j+1}}{T_{j+1} - T_j} + \frac{1}{2},$$

where  $p \geq 2$ . The function  $w$  is a smooth, increasing, bijection on each of the intervals  $[T_j, T_{j+1}]$  for  $1 \leq j \leq P$ , with  $w^{(k)}(T_j) = w^{(k)}(T_{j+1}) =$

0 for  $1 \leq k \leq p - 1$ . We then define the new parametrization

$$x(t) = (x_1(w(t)), x_2(w(t)))$$

extended by  $2\pi$ -periodicity, if needed, to any  $t \in \mathbb{R}$ .

A central issue that collocation discretizations of the integral equations CFIEFK (3.15), CFIESK (3.16) and SCFIE (3.18) is confronted with is the possibly unbounded nature of their solutions at corners. In what follows, we deal with this issue by introducing new *weighted* unknown densities, defined as

$$(5.2) \quad \gamma_N^{1,w} u^t(t) := (\gamma_N u^t)(\mathbf{x}(t)) |\mathbf{x}'(t)|$$

for equations CFIEFK (3.15) and CFIESK (3.16), as well as a new *weighted* unknown density defined as

$$(5.3) \quad \mu^w(t) := \mu(\mathbf{x}(t)) |\mathbf{x}'(t)|$$

for the equation SCFIE (3.18).

According to the classical theory of singularities of solutions of elliptic problems in non-smooth domains, the solutions of the integral equations CFIEFK (3.15), CFIESK (3.16), CFIER (3.17) and SCFIE (3.18) exhibit corner singularities [13]. In the case of smooth incident fields  $u^{\text{inc}}$  (e.g., plane wave incidence) we have that  $(\gamma_D u^{\text{inc}}, \gamma_N u^{\text{inc}}) \in H^1(\Gamma) \times L^2(\Gamma)$ . Given that, by Theorem 4.5, the operators CSK (and/or CFK) are invertible in the space  $H^1(\Gamma) \times L^2(\Gamma)$  we obtain that  $(\gamma_D u^t, \gamma_N u^t) \in H^1(\Gamma) \times L^2(\Gamma)$ . Consequently, it follows from Sobolev embedding theorems that  $\gamma_D u^t$  is Hölder continuous on  $\Gamma$ . Also, given that, by Theorem 4.8, the operators SIE are invertible in  $L^2(\Gamma)$ , we obtain that the solution  $\mu$  of the SCFIE equation (3.18) belongs to  $L^2(\Gamma)$ . In conclusion, in the case of smooth incident fields  $u^{\text{inc}}$ , the  $L^2$  integrable corner singularities of  $\gamma_N u^t$  and  $\mu$  are mollified by the corner polynomially vanishing weights  $|\mathbf{x}'|$  for large enough values of the exponent  $p$  of the sigmoid transform. Indeed, for large enough values of  $p$ , the  $2\pi$  periodic functions  $\gamma_N^{1,w} u^t$  and  $\mu^w$  vanish at  $T_j$  for all  $1 \leq j \leq P$  and are regular enough.

**Remark 5.1.** More precise statements can be made about the nature of the functions  $\gamma_N^{1,w} u^t$  and  $\mu^w$  if we resort to the corner asymptotic behavior of  $\gamma_N^{1,w} u^t$ . Indeed, it was shown in [13] that, under the assumptions of smooth incident fields and  $\rho \neq 1$ , the Neumann trace

$\gamma_N^{1,w} u^t$  behaves as  $\gamma_N^{1,w} u^t \sim c_j r_j^{\lambda_j}$ ,  $r_j \rightarrow 0$ ,  $-1 < \lambda_j < 0$ ,  $c_j \in \mathbb{C}$  where  $r_j$  denotes the radial distance to the corner  $\mathbf{x}_j$  and  $\lambda_j$  is a solution of the transcendental equation

$$(5.4) \quad \frac{\sin(\lambda_j \pi - (1 + \lambda_j)\theta_j)}{\sin(\lambda_j \pi)} = \mp \frac{\rho + 1}{\rho - 1},$$

where  $\theta_j$  is the aperture of the interior angle at the corner  $\mathbf{x}_j$ . In the case of smooth incident fields and  $\rho = 1$ , it can be shown that  $\gamma_N^{1,w} u$  is actually more regular. Similar arguments allow us to obtain identical exponents in the corner asymptotic behavior of the solution  $\mu^w$  of the SIE equations (3.18).

In what follows, we introduce the graded-parameterized version of the four boundary integral operators of the Helmholtz equation. In light of the above discussion on the regularity of  $\gamma_D u$ ,  $\gamma_N^{1,w} u^t$  and  $\mu^w$ , we consider the cases when these boundary integral operators act on two types of  $2\pi$  periodic densities: (1) we assume that  $\varphi \in C^\alpha[0, 2\pi]$  where  $\alpha$  is large enough and in addition  $\varphi(t)$  behaves like  $|t - T_j|^r$ ,  $r > 0$ , for all  $1 \leq j \leq P + 1$ ; and (2) we assume that  $\psi \in C^{0,\beta}[0, 2\pi]$ ,  $0 < \beta < 1$  is a Hölder continuous density. We start by defining the parametrized single layer operator in the form

$$(5.5) \quad (S_k \varphi)(t) := \int_0^{2\pi} G_k(\mathbf{x}(t) - \mathbf{x}(\tau)) \varphi(\tau) d\tau.$$

Next, we define the parametrized double layer operator in the form

$$(5.6) \quad (K_k \psi)(t) := \int_0^{2\pi} \frac{\partial G_k(\mathbf{x}(t) - \mathbf{x}(\tau))}{\partial \mathbf{n}(\mathbf{x}(\tau))} |\mathbf{x}'(\tau)| \psi(\tau) d\tau.$$

and the parametrized weighted adjoint of the double layer operator as

$$(5.7) \quad (K_k^\top, w \varphi)(t) := \int_0^{2\pi} |\mathbf{x}'(t)| \frac{\partial G_k(\mathbf{x}(t) - \mathbf{x}(\tau))}{\partial \mathbf{n}(\mathbf{x}(t))} \varphi(\tau) d\tau.$$

Finally, we defined the parametrized weighted hypersingular operator as:

$$(5.8) \quad \begin{aligned} (N_k^w \psi)(t) &:= k^2 \int_0^{2\pi} G_k(\mathbf{x}(t) - \mathbf{x}(\tau)) |\mathbf{x}'(t)| |\mathbf{x}'(\tau)| \\ &\quad (\mathbf{n}(\mathbf{x}(t)) \cdot \mathbf{n}(\mathbf{x}(\tau))) \psi(\tau) d\tau \\ &\quad + \text{PV} \int_\Gamma |\mathbf{x}'(t)| (\partial_s G_k)(\mathbf{x}(t) - \mathbf{x}(\tau)) \psi'(\tau) d\tau. \end{aligned}$$

Having defined parametrized weighted versions of the boundary integral operators associated with the Helmholtz equation, next we present parametrized weighted versions of the integral equations CFIEFK (3.15), CFIESK (3.16), CFIER (3.17) and SCFIE (3.18).

In the case of the *physical* formulations CFIEFK (3.15) and CFIESK (3.16), we introduce the additional notation (see equation (5.2))

$$\begin{aligned}
 \gamma_D u(t) &:= (\gamma_D u)(\mathbf{x}(t)), \\
 \gamma_D u^{\text{inc}}(t) &:= u^{\text{inc}}(\mathbf{x}(t)), \\
 \gamma_N^w u^{\text{inc}}(t) &:= (\gamma_N u^{\text{inc}})(\mathbf{x}(t))|\mathbf{x}'(t)|,
 \end{aligned}
 \tag{5.9}$$

We multiply both sides of the second equations in formulations CFIEFK (3.15) and CFIESK (3.16) by the term  $|\mathbf{x}'(t)|$ , and we obtain

$$\begin{aligned}
 \text{CFK}^w \begin{bmatrix} \gamma_D u^t \\ \gamma_N^{1,w} u^t \end{bmatrix} &:= \begin{bmatrix} -(K_1 + K_2) & (\rho^{-1}S_2 + S_1) \\ -(N_1^w + \rho N_2^w) & (K_1^{\top,w} + K_2^{\top,w}) \end{bmatrix} \begin{bmatrix} \gamma_D u^t \\ \gamma_N^{1,w} u^t \end{bmatrix} \\
 &= \begin{bmatrix} \gamma_D u^{\text{inc}} \\ \gamma_N^w u^{\text{inc}} \end{bmatrix},
 \end{aligned}
 \tag{5.10}$$

and respectively,

$$\begin{aligned}
 \text{CSK}^w \begin{bmatrix} \gamma_D u^t \\ \gamma_N^{1,w} u^t \end{bmatrix} &:= \left( \frac{\rho^{-1} + 1}{2} \begin{bmatrix} I & \\ & I \end{bmatrix} \right. \\
 &\quad \left. + \begin{bmatrix} (K_2 - \rho^{-1}K_1) & \rho^{-1}(S_1 - S_2) \\ -(N_1^w - N_2^w) & (K_1^{\top,w} - \rho^{-1}K_2^{\top,w}) \end{bmatrix} \right) \begin{bmatrix} \gamma_D u^t \\ \gamma_N^{1,w} u^t \end{bmatrix} \\
 &= \begin{bmatrix} \rho^{-1} \gamma_D u^{\text{inc}} \\ \gamma_N^w u^{\text{inc}} \end{bmatrix}.
 \end{aligned}
 \tag{5.11}$$

The weighted version of the CFIER formulations (3.17) can be written as

$$\begin{aligned}
 \text{GFK}^w \begin{bmatrix} \gamma_D u^t \\ \gamma_N^{1,w} u^t \end{bmatrix} &:= \left( \frac{\rho}{\rho + 1} \text{CSK}^w + \frac{2}{1 + \rho} \begin{bmatrix} & S_\kappa \\ -\rho N_\kappa^w & \end{bmatrix} \text{CFK}^w \right) \begin{bmatrix} \gamma_D u^t \\ \gamma_N^{1,w} u^t \end{bmatrix} \\
 &= \frac{1}{\rho + 1} \begin{bmatrix} I & 2S_\kappa \\ -2\rho N_\kappa^w & \rho I \end{bmatrix} \begin{bmatrix} \gamma_D u^{\text{inc}} \\ \gamma_N^w u^{\text{inc}} \end{bmatrix}, \quad 0 \leq t < 2\pi.
 \end{aligned}$$

In addition, with efficiency considerations in mind, we also consider an alternative version of the regularized formulations in which the operators  $S_\kappa$  and  $N_\kappa^w$  are replaced by appropriate Fourier multipliers, which are the principal symbols of the former operators in the sense of pseudodifferential operators [4]. Specifically, we use the following Fourier multipliers:

$$(5.12) \quad \begin{aligned} (PS_{N,\kappa}^w \phi)(\mathbf{x}(t)) &= |\mathbf{x}'(t)| \sum_{n \in \mathbb{Z}} \sigma_{N,\kappa}(n) \widehat{\phi}(n) e^{i n t}, \\ \sigma_{N,\kappa}(\xi) &= -\frac{1}{2} \sqrt{|\xi|^2 - \kappa^2}, \end{aligned}$$

and

$$(5.13) \quad \begin{aligned} (PS_{S,\kappa} \psi)(\mathbf{x}(t)) &= \sum_{n \in \mathbb{Z}} \sigma_{S,\kappa}(n) \widehat{\psi}(n) e^{i n t}, \\ \sigma_{S,\kappa}(\xi) &= \frac{1}{2\sqrt{|\xi|^2 - \kappa^2}}, \end{aligned}$$

acting on  $2\pi$ -periodic densities  $\phi$  and  $\psi$ , where  $\widehat{\phi}(n)$  and  $\widehat{\psi}(n)$  are the Fourier coefficients of the functions  $\phi$  and  $\psi$ , respectively. With the aid of these Fourier multipliers we define the weighted Principal Symbol CFIER formulation (CFIERPS)

$$(5.14) \quad \begin{aligned} & \text{PSGFK}^w \begin{bmatrix} \gamma_D u^t \\ \gamma_N^{1,w} u^t \end{bmatrix} \\ & := \left( \frac{\rho}{\rho+1} \text{CSK}^w + \frac{2}{1+\rho} \begin{bmatrix} & PS_{S,\kappa} \\ -\rho PS_{N,\kappa}^w & \end{bmatrix} \right) \begin{bmatrix} \gamma_D u^t \\ \gamma_N^{1,w} u^t \end{bmatrix} \\ & = \frac{1}{\rho+1} \begin{bmatrix} I & 2PS_{S,\kappa} \\ -2\rho PS_{N,\kappa}^w & \rho I \end{bmatrix} \begin{bmatrix} \gamma_D u^{\text{inc}} \\ \gamma_N^w u^{\text{inc}} \end{bmatrix}, \quad 0 \leq t < 2\pi. \end{aligned}$$

We note that we did not establish the well-posedness of the CFIERPS formulations. Nevertheless, we give plenty of numerical evidence in subsection 5.4 that the CFIERPS formulations are robust and computationally advantageous.

Finally, in order to derive weighted parametrized versions of the SCFIE equation, we consider the same layer representation of the fields  $u^2$  and  $u^1$ , but a weighted Burton-Miller type combination of the form

$$(\gamma_N^{1,w} u^1 - i\eta \gamma_D^1 u^1) - (\rho \gamma_N^{2,w} u^2 - i\eta \gamma_D^2 u^2) = -\gamma_N^w u^{\text{inc}} + i\eta \gamma_D u^{\text{inc}}$$

( $\gamma_N^{j,w} u^j$  for  $j = 1, 2$  are defined as in (5.2)) to lead to the following weighted boundary integral equation:

$$(5.15) \quad -\frac{1+\rho}{2}\mu^w + \mathbf{K}^w \mu^w - i\eta \mathbf{S}^w \mu^w = \gamma_N^w u^{\text{inc}} - i\eta \gamma_D u^{\text{inc}}, \quad \text{on } [0, 2\pi],$$

$$\eta \in \mathbb{R} \quad \eta \neq 0,$$

where

$$\mathbf{K}^w = -K_2^{\top,w}(\rho I - 2K_2^{\top,w}) - \rho K_1^{\top,w}(I + 2K_2^{\top,w}) + 2(N_1^w - N_2^w)S_2$$

and

$$\mathbf{S}^w = -\rho S_1(I + 2K_2^{\top,w}) - (I - 2K_1)S_2.$$

**Remark 5.2.** It is possible to define more general weighted unknowns if we replace the weight  $|\mathbf{x}'|$  by  $|\mathbf{x}'|^\delta$ ,  $\delta \geq 1/2$ , the new weights leading to new weighted integral equation formulations. Furthermore, it is possible to define weighted unknowns that involve the Dirichlet data, that is  $\gamma_D^w u(t) := u(\mathbf{x}(t))|\mathbf{x}'(t)|^\delta$  leading again to new weighted integral equations. We note that the latter type of weighted unknowns (with  $\delta = 1/2$ ) and weighted boundary integral equations of CFIESK type were used in [15, 19].

**5.2. Nyström discretizations based on kernel splitting and trigonometric interpolation.** We use a Nyström discretization of the weighted parametrized equations (5.10)–(5.12), (5.14) and (5.15) that relies on (a) splitting of the kernels of the weighted parametrized operators into smooth and singular components, (b) trigonometric interpolation of the unknowns of these integral equations and (c) analytical expressions for the integrals of products of periodic singular and weakly singular kernels and Fourier harmonics. Several details of this method were originally introduced in [28]; for completeness, we give out the full details in what follows.

We present first a strategy to split the kernels of the weighted parametrized integral operators featured in equations (5.10)–(5.12) and (5.15) into smooth and singular components. The latter, in turn, can be expressed as products of *known* singular kernels and smooth kernels.

We assume that  $k > 0$ , and we begin by looking at the operator (5.16)

$$(S_k \varphi)(t) = \int_0^{2\pi} M_k(t, \tau) \varphi(\tau) d\tau := \int_0^{2\pi} G_k(\mathbf{x}(t) - \mathbf{x}(\tau)) \varphi(\tau) d\tau,$$

where  $\varphi$  is a sufficiently smooth  $2\pi$ -periodic function (recall that, basically,  $\varphi(t) := |\mathbf{x}'(t)| \gamma_N^1 u(\mathbf{x}(t))$ ). The kernel  $M_k(t, \tau)$  can be expressed in the form

$$M_k(t, \tau) = M_{k,1}(t, \tau) \ln \left( 4 \sin^2 \frac{t - \tau}{2} \right) + M_{k,2}(t, \tau)$$

with

$$M_{k,1}(t, \tau) := -\frac{1}{4\pi} J_0(k|\mathbf{r}|)$$

$$M_{k,2}(t, \tau) := M_k(t, \tau) - M_{k,1}(t, \tau) \ln \left( 4 \sin^2 \frac{t - \tau}{2} \right),$$

where we have denoted, for simplifying this and forthcoming expressions,

$$\mathbf{r} = \mathbf{r}(t, \tau) = \mathbf{x}(t) - \mathbf{x}(\tau).$$

Observe that the diagonal terms are given by

$$M_{k,1}(t, t) = -\frac{1}{4\pi}, \quad M_{k,2}(t, t) = \frac{i}{4} - \frac{C}{2\pi} - \frac{1}{2\pi} \ln \frac{k|\mathbf{x}'(t)|}{2},$$

where  $C \approx 0.5772$  is the Euler-Mascheroni constant.

The parametrized double layer operator, see equation (3.2), is defined as follows

$$(5.17) \quad \begin{aligned} (K_k \psi)(t) &= \int_0^{2\pi} H_k(t, \tau) \psi(\tau) d\tau \\ &:= \int_0^{2\pi} \frac{\partial G_k(\mathbf{x}(t) - \mathbf{x}(\tau))}{\partial \mathbf{n}(\mathbf{x}(\tau))} |\mathbf{x}'(\tau)| \psi(\tau) d\tau. \end{aligned}$$

We note that the kernel of the operator  $K_k$  behaves as (i)  $|t - \tau|^{-1}$  when  $t \rightarrow T_j$ ,  $t < T_j$  and  $\tau \rightarrow T_j$ ,  $\tau > T_j$  for  $2 \leq j \leq P$ , and as (ii)  $(|t - \tau| \bmod 2\pi)^{-1}$  when  $t \rightarrow T_1 = 0$  and  $\tau \rightarrow T_{P+1} = 2\pi$  (that is, when  $\mathbf{x}(t)$  and  $\mathbf{x}(\tau)$  approach a corner from different sides). Thus, the integral in the definition of the operator  $K_k$  should be understood in the sense of the Cauchy principal value integral. However, for Hölder continuous densities  $\psi$ , it is possible to recast the operators  $K_k$  into an equivalent

form that features operators that involve integrable expressions only [22]. In order to do so, we express  $K_k$  in the form (5.18)

$$\begin{aligned} (K_k\psi)(t) &= \int_0^{2\pi} \frac{\partial}{\partial \mathbf{n}(\mathbf{x}(\tau))} [G_k(\mathbf{x}(t) - \mathbf{x}(\tau)) - G_0(\mathbf{x}(t) - \mathbf{x}(\tau))] \\ &\quad |\mathbf{x}'(\tau)|\psi(\tau) d\tau \\ &\quad + \int_0^{2\pi} \frac{\partial G_0(\mathbf{x}(t) - \mathbf{x}(\tau))}{\partial \mathbf{n}(\mathbf{x}(\tau))} |\mathbf{x}'(\tau)|(\psi(\tau) - \psi(t)) d\tau \\ &\quad + \psi(t) \int_0^{2\pi} \frac{\partial G_0(\mathbf{x}(t) - \mathbf{x}(\tau))}{\partial \mathbf{n}(\mathbf{x}(\tau))} |\mathbf{x}'(\tau)| d\tau. \end{aligned}$$

We first note that

$$\int_0^{2\pi} \frac{\partial G_0(\mathbf{x}(t) - \mathbf{x}(\tau))}{\partial \mathbf{n}(\mathbf{x}(\tau))} |\mathbf{x}'(\tau)| d\tau = \begin{cases} -\frac{1}{2} & \text{if } t \in [0, 2\pi] \setminus \{T_1, \dots, T_P\}, \\ -\frac{1}{2\pi}\theta_j & \text{if } t = T_j, 1 \leq j \leq P, \end{cases}$$

where  $\theta_j$  is the inner angle of the  $j$ th corner. For the second integral, and since we have assumed  $\psi$  to be Hölder continuous, the integrand is weakly singular. Finally, in the kernel of the first integral operator in (5.18), we find the function

$$H_k(t, \tau) = \left[ \frac{\partial G_k}{\partial \mathbf{n}(\mathbf{x}(\tau))} \right] (\mathbf{r}) |\mathbf{x}'(\tau)| = \frac{ik}{4} \boldsymbol{\nu}(\tau) \cdot \mathbf{r} \frac{H_1^{(1)}(k|\mathbf{r}|)}{|\mathbf{r}|},$$

where

$$\boldsymbol{\nu}(\tau) := \mathbf{n}(\mathbf{x}(\tau))|\mathbf{x}'(\tau)| = w'(\tau)(x_2'(w(\tau)), -x_1'(w(\tau))).$$

We have, in addition, the decomposition

$$H_k(t, \tau) = H_{k,1}(t, \tau) \ln \left( 4 \sin^2 \frac{t - \tau}{2} \right) + H_{k,2}(t, \tau),$$

where

$$\begin{aligned} H_{k,1}(t, \tau) &:= -\frac{k}{4\pi} \boldsymbol{\nu}(\tau) \cdot \mathbf{r} \frac{J_1(k|\mathbf{r}|)}{|\mathbf{r}|} \\ H_{k,2}(t, \tau) &:= H_k(t, \tau) - H_{k,1}(t, \tau) \ln \left( 4 \sin^2 \frac{t - \tau}{2} \right), \end{aligned}$$

which have the diagonal terms

$$H_{k,1}(t, t) = 0, \quad H_{k,2}(t, t) = \frac{1}{4\pi} \frac{\boldsymbol{\nu}(t) \cdot \mathbf{x}''(t)}{|\mathbf{x}'(t)|^2}.$$

It can be easily seen that the second function in the kernel of the first integral operator in (5.18) is given by

$$\begin{aligned} H_0(t, \tau) &= \left[ \frac{\partial G_0}{\partial \mathbf{n}(\mathbf{x}(\tau))} \right](\mathbf{r}) |\mathbf{x}'(\tau)| = \frac{1}{2\pi} \frac{\boldsymbol{\nu}(\tau) \cdot \mathbf{r}}{|\mathbf{r}|^2}, \\ H_0(t, t) &= \frac{1}{4\pi} \frac{\boldsymbol{\nu}(t) \cdot \mathbf{x}''(t)}{|\mathbf{x}'(t)|^2}, \end{aligned}$$

and thus  $H_{k,2}(t, t) - H_0(t, t)$ , appearing in the first term in (5.18), can be defined even at corner points where  $|\mathbf{x}'(t)| = 0$ .

The graded-parametrized adjoint of the double layer, cf., definition (3.3), is given by

$$\begin{aligned} (K_k^{\top, w} \varphi)(t) &= \int_0^{2\pi} H_k^{\top}(t, \tau) \varphi(\tau) d\tau \\ (5.19) \quad &:= \int_0^{2\pi} |\mathbf{x}'(t)| \frac{\partial G_k(\mathbf{x}(t) - \mathbf{x}(\tau))}{\partial \mathbf{n}(\mathbf{x}(t))} \varphi(\tau) d\tau. \end{aligned}$$

Here,

$$H_k^{\top}(t, \tau) = \frac{ik}{4} \boldsymbol{\nu}(t) \cdot \mathbf{r} \frac{H_1^{(1)}(k|\mathbf{r}|)}{|\mathbf{r}|}.$$

The kernel  $H_k^{\top}(t, \tau)$  can be expressed in the form

$$H_k^{\top}(t, \tau) = H_{k,1}^{\top}(t, \tau) \ln \left( 4 \sin^2 \frac{t - \tau}{2} \right) + H_{k,2}^{\top}(t, \tau)$$

with

$$\begin{aligned} H_{k,1}^{\top}(t, \tau) &:= -\frac{k}{4\pi} \boldsymbol{\nu}(t) \cdot \mathbf{r} \frac{J_1(k|\mathbf{r}|)}{|\mathbf{r}|} \\ H_{k,2}^{\top}(t, \tau) &:= H_k^{\top}(t, \tau) - H_{k,1}^{\top}(t, \tau) \ln \left( 4 \sin^2 \frac{t - \tau}{2} \right) \end{aligned}$$

and

$$H_{k,1}^{\top}(t, t) = 0, \quad H_{k,2}^{\top}(t, t) = \frac{1}{4\pi} \frac{\boldsymbol{\nu}(t) \cdot \mathbf{x}''(t)}{|\mathbf{x}'(t)|^2}.$$

A simple calculation shows that  $H_{k,2}^\top(t, t)$  is infinite whenever  $|\mathbf{x}'(t)| = 0$ , that is,  $w'(t) = 0$ .

**Remark 5.3.** Notice that although  $H_{k,2}^\top$  is unbounded in and around corners, the product  $H_{k,2}^\top(t, t)\varphi(t)$  still vanishes at corners. Indeed, in a neighborhood of a corner, say  $t \sim T_j$  the function  $\varphi$  behaves as  $\varphi(t) \sim c_j[w'(t)]^{1+\lambda_j}$ ,  $-1/2 < \lambda_j$ . A careful inspection of the singularity of  $H_{k,2}^\top(t, t)$  reveals that this expression behaves as  $w''(t)/w'(t)$  and thus the product  $H_{k,2}^\top(t, t)\varphi(t) \sim c_j w''(t)[w'(t)]^{\lambda_j}$ . Given that  $w(t) \sim |t - T_j|^p$ ,  $t \rightarrow T_j$ , we see that the latter product is regular enough for  $t \rightarrow T_j$  provided that  $p$  is sufficiently large.

Finally, for the graded-parametrized version of the hypersingular operator  $N_k$ , we add and subtract  $(1/4\pi) \ln(4 \sin^2((t - \tau)/2))$  to get

$$\begin{aligned} (N_k^w \psi)(t) &= -\text{PV} \frac{1}{4\pi} \int_0^{2\pi} \cot \frac{t - \tau}{2} \psi'(\tau) \, d\tau \\ &\quad + \int_0^{2\pi} Q_k(t, \tau) \psi(\tau) \, d\tau + \int_0^{2\pi} D_k(t, \tau) \psi'(\tau) \, d\tau, \end{aligned}$$

with

$$\begin{aligned} Q_k(t, \tau) &:= k^2 M_k(t, \tau) (\mathbf{x}'(t) \cdot \mathbf{x}'(\tau)) \\ D_k(t, \tau) &:= \frac{\partial}{\partial t} \left( \frac{1}{4\pi} \ln \left( \sin^2 \frac{t - \tau}{2} \right) + M_k(t, \tau) \right). \end{aligned}$$

Note that we have used

$$|\mathbf{x}'(t)| |\mathbf{x}'(\tau)| \mathbf{n}(\mathbf{x}(t)) \cdot \mathbf{n}(\mathbf{x}(\tau)) = \mathbf{x}'(t) \cdot \mathbf{x}'(\tau).$$

The kernel  $Q_k$  can be treated similarly to the kernel  $M_k$ . On the other hand, a simple calculation gives that

$$D_k(t, \tau) = D_{k,1}(t, \tau) \ln \left( 4 \sin^2 \frac{t - \tau}{2} \right) + D_{k,2}(t, \tau),$$

where

$$\begin{aligned} D_{k,1}(t, \tau) &:= \frac{k}{4\pi} \mathbf{x}'(t) \cdot \mathbf{r} \frac{J_1(k|\mathbf{r}|)}{|\mathbf{r}|} \\ D_{k,2}(t, \tau) &:= D_k(t, \tau) - D_{k,1}(t, \tau) \ln \left( 4 \sin^2 \frac{t - \tau}{2} \right) \end{aligned}$$

have diagonal terms

$$D_{k,1}(t, t) = 0, \quad D_{k,2}(t, t) = \frac{1}{4\pi} \frac{\mathbf{x}'(t) \cdot \mathbf{x}''(t)}{|\mathbf{x}'(t)|^2}.$$

Again,  $D_{k,2}(t, t)$  is infinite at corners, but the trapezoidal rule can still be applied since that term is multiplied by  $\psi'(t)$  which vanishes at the corners; this requires the same type of justification used in Remark 5.3.

We note that the weighted integral equations CFIESK (5.11) and SCFIE (5.15) feature the difference operator  $N_1^w - N_2^w$ . While this difference can be performed directly using the methodology presented above for the evaluation of the operators  $N_1^w$  and  $N_2^w$ , a more advantageous approach relies on the methods developed by Kress in [23] for the evaluation of operators  $N_k^w - N_0^w$ , where  $N_0^w$  is the weighted hypersingular operator corresponding to wavenumber  $k = 0$ . The latter methodology consists of expressing the graded-parametrized operators, constructed from equation (3.4) instead, as

$$(5.20) \quad \begin{aligned} & ([N_k^w - N_0^w]\psi)(y) \\ &= - \int_0^{2\pi} (\boldsymbol{\nu}(t))^\top \nabla^2(G_k - G_0)(\mathbf{x}(t) - \mathbf{x}(\tau))(t, \tau) \boldsymbol{\nu}(\tau) \psi(\tau) d\tau \end{aligned}$$

We have (see the proof of Lemma 4.2) that

$$\begin{aligned} \nabla^2(G_k - G_0)(\mathbf{r}) &= -\frac{ik^2}{4} H_0^{(1)}(k|\mathbf{r}|) \frac{1}{|\mathbf{r}|^2} \mathbf{r} \mathbf{r}^\top \\ &\quad + \left( \frac{i}{4} H_1^{(1)}(k|\mathbf{r}|) k|\mathbf{r}| - \frac{1}{2\pi} \right) \left( \frac{2}{|\mathbf{r}|^4} \mathbf{r} \mathbf{r}^\top - \frac{1}{|\mathbf{r}|^2} I \right) \\ &= L_{1,k,0}(t, \tau) \ln \left( \sin^2 \frac{t - \tau}{2} \right) + L_{2,k,0}(t, \tau), \end{aligned}$$

where  $I$  is the  $2 \times 2$  identity matrix, and

$$\begin{aligned} L_{1,k,0}(t, \tau) &= \frac{k}{4\pi} \left[ \frac{J_1(k|\mathbf{r}|)}{|\mathbf{r}|} I + \frac{1}{|\mathbf{r}|^2} \left( kJ_0(k|\mathbf{r}|) - 2 \frac{J_1(k|\mathbf{r}|)}{|\mathbf{r}|} \right) \mathbf{r} \mathbf{r}^\top \right] \\ L_{2,k,0}(t, \tau) &:= \nabla^2(G_k - G_0)(\mathbf{r}) - L_{1,k,0}(t, \tau) \ln \left( \sin^2 \frac{t - \tau}{2} \right) \end{aligned}$$

satisfies

$$L_{1,k,0}(t, t) = \frac{k^2}{8\pi} I,$$

$$L_{2,k,0}(t, t) = k^2 \left[ \frac{1}{4\pi} \ln \left( \frac{k|\mathbf{x}'(t)|}{2} \right) - \frac{i}{8} + \frac{2C - 1}{8\pi} \right] I + \frac{k^2}{4\pi} \frac{1}{|\mathbf{x}'(t)|^2} \mathbf{x}'(t) (\mathbf{x}'(t))^\top.$$

It then follows that

$$(\boldsymbol{\nu}(t))^\top (\nabla^2(G_k - G_0)(\mathbf{r})) \boldsymbol{\nu}(\tau) = L_{1,k}(t, \tau) \ln \left( 4 \sin^2 \frac{t - \tau}{2} \right) + L_{2,k}(t, \tau)$$

with diagonal terms

$$L_{1,k}(t, t) = \frac{k^2}{8\pi} |\mathbf{x}'(t)|^2, \\ L_{2,k}(t, t) = k^2 \left[ \frac{1}{4\pi} \ln \left( \frac{k|\mathbf{x}'(t)|}{2} \right) - \frac{i}{8} + \frac{2C - 1}{8\pi} \right] |\mathbf{x}'(t)|^2,$$

that are bounded even around corner points where  $\mathbf{x}'(t) = 0$ . Thus, we can apply the procedure above for the graded-parametrized operator  $N_{k_1}^w - N_{k_2}^w = (N_{k_1}^w - N_0^w) - (N_{k_2}^w - N_0^w)$ , so that we are led to integral operators whose kernels are of the form

$$L_{k_1, k_2}(t, \tau) := [L_{1, k_1}(t, \tau) - L_{1, k_2}(t, \tau)] \ln \left( 4 \sin^2 \frac{t - \tau}{2} \right) + [L_{2, k_1}(t, \tau) - L_{2, k_2}(t, \tau)].$$

The splitting techniques presented above can be adapted for evaluation of the operators  $S_\kappa$  and  $N_\kappa^w$  with  $\Im(\kappa) > 0$  using additional smooth cutoff function supported in neighborhoods of the target points  $t$  according to the procedures introduced in [4].

**5.3. Trigonometric interpolation.** Next we describe a Nyström method based on trigonometric interpolation that closely follows the quadrature method introduced by Kress in [23], which in turn relies on the logarithmic quadrature methods introduced by Kussmaul [26] and Martensen [29]. The main idea is to use global trigonometric interpolation of the quantities  $\gamma_D u^t$ ,  $\gamma_N^{1,w} u^t$  and  $\mu^w$  that are the solutions of the integral equations (5.10), (5.11) and (5.15). Given that the larger the exponent  $p$  of the sigmoidal transform is, the smoother the quantities  $\gamma_N^{1,w} u^t$  and  $\mu^w$  are, the trigonometric interpolants of these quantities converge fast with respect to the number of interpolation

points. We choose an equispaced splitting of the interval  $[0, 2\pi]$  into  $2n$  points. We choose  $T_j$  such that  $T_{j+1} - T_j$  are proportional (with the same constant of proportionality) to the lengths of the arcs of  $\Gamma$  from  $\mathbf{x}_j$  to  $\mathbf{x}_{j+1}$  for all  $j$ . Consequently, the number of discretization points per subinterval  $[T_j, T_{j+1}]$ ,  $1 \leq j \leq P$ , may differ from each other. We thus consider the equispaced collocation points  $\{t_0^{(n)}, t_1^{(n)}, \dots, t_{2n-1}^{(n)}\}$  and the interpolation problem with respect to these nodal points in the space  $\mathbb{T}_n$  of trigonometric polynomials of the form

$$v(t) = \sum_{m=0}^n a_m \cos mt + \sum_{m=1}^{n-1} b_m \sin mt,$$

which is uniquely solvable [24]. We denote by  $P_n : C[0, 2\pi] \rightarrow \mathbb{T}_n$  the corresponding trigonometric polynomial interpolation operator. We use the quadrature rules [23]

(5.21)

$$\begin{aligned} \int_0^{2\pi} \ln \left( 4 \sin^2 \frac{t - \tau}{2} \right) f(\tau) d\tau &\approx \int_0^{2\pi} \ln \left( 4 \sin^2 \frac{t - \tau}{2} \right) (P_n f)(\tau) d\tau \\ &= \sum_{i=0}^{2n-1} R_i^{(n)}(t) f(t_i^{(n)}), \end{aligned}$$

where the expressions  $R_i^{(n)}(t)$  are given by

$$R_i^{(n)}(t) = -\frac{2\pi}{n} \sum_{m=1}^{n-1} \frac{1}{m} \cos m(t - t_i^{(n)}) - \frac{\pi}{n^2} \cos n(t - t_i^{(n)}).$$

We also use the trapezoidal rule

(5.22)

$$\int_0^{2\pi} f(\tau) d\tau \approx \int_0^{2\pi} (P_n f)(\tau) d\tau = \frac{\pi}{n} \sum_{i=0}^{2n-1} f(t_i^{(n)}).$$

Finally, we have the quadrature rule [23]:

(5.23)

$$\begin{aligned} \frac{1}{4\pi} \int_0^{2\pi} \cot \frac{\tau - t}{2} f'(\tau) d\tau &\approx \frac{1}{4\pi} \int_0^{2\pi} \cot \frac{\tau - t}{2} \frac{d}{d\tau} [(P_n f)(\tau)] d\tau \\ &= \sum_{i=0}^{2n-1} T_i^{(n)}(t) f(t_i^{(n)}), \end{aligned}$$

where

$$T_i^{(n)}(t) = -\frac{1}{2n} \sum_{m=1}^{n-1} m \cos m(t - t_i^{(n)}) - \frac{1}{4} \cos n(t - t_i^{(n)}).$$

The derivatives of the densities needed for evaluation of the operators  $N_k^w$  and  $N_\kappa^w$  are affected by differentiation of the global trigonometric interpolant of the densities. This can be pursued either by means of fast fourier transforms (FFTs) or by using the Fourier differentiation matrix  $D^{(n)}$ , whose entries are given by

$$D^{(n)}(i, j) = \frac{1}{2}(-1)^{i+j} \cot\left(\frac{(i-j)\pi}{n}\right), \quad i \neq j$$

and  $D^{(n)}(i, i) = 0$ .

Finally, given that the values of  $\gamma_N^{1,w} u^t$  and  $\mu^w$  vanish at corner points, the terms in the boundary integral equations that feature these quantities are not collocated at corner points. Alternatively, this issue can be bypassed altogether by shifting the mesh  $t_j^{(n)}$  by  $h/2$ , where  $h$  is the meshsize. All of the interpolatory quadratures presented above still apply for the shifted meshes. Finally, the Fourier multipliers  $PS_{S,\kappa}^w$  and  $PS_{N,\kappa}^w$  defined in equations (5.12) and (5.13) can easily be evaluated using trigonometric interpolation and FFTs.

**5.4. Numerical results.** We present in this section a variety of numerical results that demonstrate the properties of the various formulations considered in this text. Solutions of the linear systems arising from the Nyström discretizations of the transmission integral equations described in Section 5 are obtained by means of the fully complex, un-restarted version of the iterative solver GMRES [35]. For the case of the regularized formulations we present choices of the complex wavenumber  $\kappa$  in each of the cases considered; our extensive numerical experiments suggest that these values of  $\kappa$  lead to nearly optimal numbers of GMRES iterations by reaching desired (small) GMRES relative residuals. We also present in each table the values of the GMRES relative residual tolerances used in the numerical experiments.

We present scattering experiments concerning the following two Lipschitz geometries, see Figure 1; (a) A square whose sides equal to 4, and (b) a U-shaped scatterer of sides equal to 4 and indentation equal to 2. For every scattering experiment, we consider plane-wave incidence

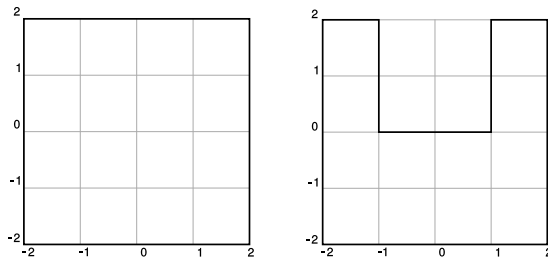


FIGURE 1. Domains for our numerical tests: (a) square; (b) U-shaped domain.

$u^{\text{inc}}$  of direction  $(0, -1)$ , and we present maximum far-field errors, that is, we choose sufficiently many directions  $\mathbf{x}/|\mathbf{x}|$  (1,024 directions have been used in our computations) and, for each direction, we compute the far-field amplitude  $u_\infty^1(\hat{\mathbf{x}})$  defined as

$$(5.24) \quad u^1(\mathbf{x}) = \frac{e^{ik_1|\mathbf{x}|}}{\sqrt{|\mathbf{x}|}} \left( u_\infty^1(\hat{\mathbf{x}}) + \mathcal{O}\left(\frac{1}{|\mathbf{x}|}\right) \right), \quad |\mathbf{x}| \rightarrow \infty.$$

The maximum far-field errors were evaluated through comparisons of the numerical solutions  $u_\infty^{1,\text{calc}}$  corresponding to either formulation with reference solutions  $u_\infty^{1,\text{ref}}$  by means of the relation

$$(5.25) \quad \varepsilon_\infty = \max |u_\infty^{1,\text{calc}}(\hat{\mathbf{x}}) - u_\infty^{1,\text{ref}}(\hat{\mathbf{x}})|.$$

The latter solutions  $u_\infty^{1,\text{ref}}$  were produced using solutions corresponding with refined discretizations based on the formulation CFIESK with GMRES residuals of  $10^{-12}$  for all geometries. Besides far field errors, we display the numbers of iterations required by the GMRES solver to reach relative residuals that are specified in each case. In the numerical experiments, we used discretizations ranging from 6 to 12 discretization points per wavelength, for frequencies  $k_1$  and  $k_2$  in the medium- to the high-frequency range corresponding to scattering problems of sizes ranging from 2.5 to 40.8 wavelengths. The Unknowns column (X) in all tables displays the numbers of unknowns used in each case, which equals the value  $4n$  defined in Section 5 for the weighted CFIEFK, CFIESK, CFIER and CFIERPS formulations, and  $2n$  for the weighted SCFIE formulation. As a reminder that the SCFIE formulations require half the number of unknowns required by each of the other

formulations, we denote the former by SCFIE\* in the tables. Following common practice [3], we used the CFIEFK operators as their own preconditioners, and we denote these by CFIEFK<sup>2</sup>. We note that, in this case, the computational time required to perform a matrix-vector product corresponding to the CFIEFK<sup>2</sup> formulation is double that related to the CFIEFK formulation.

We start by presenting the high-order convergence of our Nyström solvers in Tables 1–4. We have used sigmoid transforms with a value  $p = 3$  for all formulations but SCFIE, in which case we used  $p = 4$ . The need for a different value of  $p$  for the latter formulations can be attributed to the more singular nature of the solutions of these equations. As can be seen, solvers based on the CFIESK formulations are the most accurate on account of the fact that they do not require numerical differentiation. Tables 1, 6, 10 ( $\rho = 1$ ) and 3, 8 ( $\rho = k_1^2/k_2^2$ ) show the CFIEFK<sup>2</sup>, CFIESK, SCFIE and CFIERPS formulations for the square geometry. Tables 2, 7, 11 ( $\rho = 1$ ) and 4, 9 ( $\rho = k_1^2/k_2^2$ ) show the CFIEFK<sup>2</sup>, CFIESK, SCFIE and CFIERPS formulations for the U-shaped geometry. In Tables 1–4,  $k_1 = 1$  and  $k_2 = 4$ . In all tables, except Tables 10 and 11, for the regularized formulations CFIER and CFIERPS,  $\kappa = (k_1 + k_2)/2 + i k_1$ . In Tables 10 and 11, for the regularized formulations CFIER and CFIERPS,  $\kappa = (k_1 + k_2)/2 + i 4$ . In Tables 1–4, the GMRES residual was set equal to  $10^{-12}$ . In Tables 6–10, the GMRES residual was set equal to  $10^{-4}$ . Unknowns are represented by X. In the SCFIE formulation, we selected  $\eta = k_1$ .

In Table 5, we present computational times required by a matrix-vector product for each of the formulations CFIEFK, CFIESK, SCFIE, CFIER and CFIERPS. The computational times presented were delivered by a MATLAB implementation of the Nyström discretization on a MacBookPro machine with  $2 \times 2.3$  GHz Quad-core Intel i7 with 16 GB of memory. We present computational times for the square geometry, as the computational times required by the U-shaped geometry considered in this text are extremely similar to those for square geometry at the same levels of discretization. As can be seen from the results in Table 5, the computational times required by a matrix-vector product for the CFIEFK, CFIESK, SCFIE and CFIERPS formulations are quite similar, while the computational times required by a matrix-vector product related to the CFIER formulation are on average 1.16 times more expensive than those required by the other three formulations.

TABLE 1.

X	CFIEFK <sup>2</sup>		CFIESK		SCFIE*		CFIER		CFIERPS	
	Iter.	$\epsilon_\infty$	Iter.	$\epsilon_\infty$	Iter.	$\epsilon_\infty$	Iter.	$\epsilon_\infty$	Iter.	$\epsilon_\infty$
256	32	$6.6 \times 10^{-3}$	34	$2.4 \times 10^{-6}$	43	$3.8 \times 10^{-3}$	43	$3.2 \times 10^{-3}$	32	$3.1 \times 10^{-3}$
512	31	$8.0 \times 10^{-4}$	34	$1.8 \times 10^{-7}$	46	$5.5 \times 10^{-4}$	43	$3.9 \times 10^{-4}$	33	$3.7 \times 10^{-4}$
1024	31	$1.0 \times 10^{-4}$	34	$1.1 \times 10^{-8}$	49	$8.0 \times 10^{-5}$	47	$4.8 \times 10^{-5}$	34	$4.6 \times 10^{-5}$
2048	31	$1.2 \times 10^{-5}$	34	$4.1 \times 10^{-10}$	54	$1.2 \times 10^{-5}$	47	$6.0 \times 10^{-6}$	34	$5.8 \times 10^{-6}$

TABLE 2.

X	CFIEFK <sup>2</sup>		CFIESK		SCFIE*		CFIER		CFIERPS	
	Iter.	$\epsilon_\infty$	Iter.	$\epsilon_\infty$	Iter.	$\epsilon_\infty$	Iter.	$\epsilon_\infty$	Iter.	$\epsilon_\infty$
352	84	$4.3 \times 10^{-2}$	75	$3.7 \times 10^{-4}$	64	$1.4 \times 10^{-2}$	73	$1.7 \times 10^{-2}$	62	$1.9 \times 10^{-2}$
704	82	$5.2 \times 10^{-3}$	75	$2.2 \times 10^{-5}$	66	$1.7 \times 10^{-3}$	74	$2.1 \times 10^{-3}$	63	$2.3 \times 10^{-3}$
1408	81	$6.4 \times 10^{-4}$	75	$1.5 \times 10^{-6}$	67	$2.4 \times 10^{-4}$	75	$2.6 \times 10^{-4}$	63	$2.9 \times 10^{-4}$
2816	80	$7.9 \times 10^{-5}$	75	$9.9 \times 10^{-8}$	68	$3.7 \times 10^{-5}$	77	$3.1 \times 10^{-5}$	63	$3.7 \times 10^{-5}$

TABLE 3.

X	CFIEFK <sup>2</sup>		CFIESK		SCFIE*		CFIER		CFIERPS	
	Iter.	$\epsilon_\infty$	Iter.	$\epsilon_\infty$	Iter.	$\epsilon_\infty$	Iter.	$\epsilon_\infty$	Iter.	$\epsilon_\infty$
256	58	$9.9 \times 10^{-4}$	39	$1.5 \times 10^{-5}$	48	$2.1 \times 10^{-3}$	60	$2.0 \times 10^{-4}$	76	$4.1 \times 10^{-4}$
512	56	$1.2 \times 10^{-4}$	39	$9.0 \times 10^{-7}$	49	$3.3 \times 10^{-4}$	52	$4.5 \times 10^{-5}$	80	$5.2 \times 10^{-5}$
1024	54	$1.5 \times 10^{-5}$	37	$6.0 \times 10^{-8}$	51	$5.0 \times 10^{-5}$	57	$6.0 \times 10^{-6}$	84	$6.5 \times 10^{-6}$
2048	53	$1.9 \times 10^{-6}$	37	$4.1 \times 10^{-9}$	52	$7.6 \times 10^{-6}$	57	$7.0 \times 10^{-7}$	87	$8.2 \times 10^{-7}$

TABLE 4.

X	CFIEFK <sup>2</sup>		CFIESK		SCFIE*		CFIER		CFIERPS	
	Iter.	$\epsilon_\infty$	Iter.	$\epsilon_\infty$	Iter.	$\epsilon_\infty$	Iter.	$\epsilon_\infty$	Iter.	$\epsilon_\infty$
352	110	$6.5 \times 10^{-4}$	67	$4.8 \times 10^{-3}$	71	$5.4 \times 10^{-3}$	93	$3.5 \times 10^{-4}$	115	$2.5 \times 10^{-4}$
704	107	$1.0 \times 10^{-4}$	64	$1.1 \times 10^{-3}$	71	$8.0 \times 10^{-4}$	86	$7.2 \times 10^{-5}$	119	$3.4 \times 10^{-5}$
1408	107	$2.0 \times 10^{-5}$	64	$2.5 \times 10^{-4}$	72	$1.2 \times 10^{-4}$	88	$1.3 \times 10^{-5}$	123	$8.1 \times 10^{-5}$
2816	105	$3.9 \times 10^{-6}$	63	$5.7 \times 10^{-5}$	72	$1.7 \times 10^{-5}$	91	$4.0 \times 10^{-6}$	126	$3.4 \times 10^{-6}$

We present next in Tables 6–8 the performance of our solvers based on the five formulations considered in this text in the case of high-contrast, high-frequency configurations. We conclude, in conjunction with the results presented in Table 5, that solvers based on the SCFIE,

TABLE 5. Computational times (in seconds) for the matrix-vector products (seconds) needed by the formulations CFIEFK, CFIESK, SCFIE, CFIER and CFIERPS for the square geometry.

X	CFIEFK	CFIESK	SCFIE*	CFIER	CFIERPS
256	4.5	4.8	4.2	5.6	5.0
512	15.9	16.4	15.4	19.1	17.0
1024	59.4	63.6	64.2	73.0	63.8

TABLE 6.

X	CFIEFK <sup>2</sup>		CFIESK		SCFIE*		CFIER		CFIERPS	
	Iter.	$\epsilon_\infty$	Iter.	$\epsilon_\infty$	Iter.	$\epsilon_\infty$	Iter.	$\epsilon_\infty$	Iter.	$\epsilon_\infty$
256	18	$6.8 \times 10^{-3}$	24	$3.7 \times 10^{-4}$	25	$3.8 \times 10^{-3}$	26	$3.1 \times 10^{-3}$	21	$3.1 \times 10^{-3}$
512	24	$2.9 \times 10^{-3}$	39	$5.0 \times 10^{-4}$	37	$2.1 \times 10^{-4}$	33	$3.6 \times 10^{-3}$	32	$1.4 \times 10^{-3}$
1024	62	$4.7 \times 10^{-3}$	94	$4.0 \times 10^{-3}$	63	$1.0 \times 10^{-4}$	58	$7.5 \times 10^{-3}$	62	$1.8 \times 10^{-3}$
2048	119	$8.1 \times 10^{-3}$	162	$8.2 \times 10^{-3}$	112	$3.8 \times 10^{-4}$	102	$6.6 \times 10^{-3}$	115	$6.7 \times 10^{-3}$

TABLE 7.

$k_1$	$k_2$	X	CFIEFK <sup>2</sup>		CFIESK		SCFIE*		CFIER		CFIERPS	
			Iter.	$\epsilon_\infty$	Iter.	$\epsilon_\infty$	Iter.	$\epsilon_\infty$	Iter.	$\epsilon_\infty$	Iter.	$\epsilon_\infty$
1	4	352	52	$4.3 \times 10^{-2}$	64	$7.0 \times 10^{-4}$	45	$1.4 \times 10^{-2}$	49	$2.0 \times 10^{-2}$	44	$2.2 \times 10^{-2}$
2	8	704	76	$2.5 \times 10^{-2}$	107	$3.2 \times 10^{-3}$	78	$9.4 \times 10^{-4}$	79	$1.5 \times 10^{-2}$	75	$2.0 \times 10^{-2}$
4	16	1408	117	$8.7 \times 10^{-3}$	149	$7.7 \times 10^{-3}$	136	$3.3 \times 10^{-4}$	124	$3.9 \times 10^{-3}$	113	$4.4 \times 10^{-3}$
8	32	2816	281	$3.3 \times 10^{-2}$	351	$3.2 \times 10^{-2}$	257	$2.8 \times 10^{-4}$	257	$1.4 \times 10^{-2}$	244	$1.2 \times 10^{-2}$

TABLE 8.

$k_1$	$k_2$	X	CFIEFK <sup>2</sup>		CFIESK		SCFIE*		CFIER		CFIERPS	
			Iter.	$\epsilon_\infty$	Iter.	$\epsilon_\infty$	Iter.	$\epsilon_\infty$	Iter.	$\epsilon_\infty$	Iter.	$\epsilon_\infty$
1	4	256	30	$9.8 \times 10^{-4}$	23	$6.7 \times 10^{-5}$	28	$2.1 \times 10^{-3}$	33	$2.1 \times 10^{-4}$	47	$4.3 \times 10^{-4}$
2	8	512	53	$1.2 \times 10^{-3}$	34	$1.3 \times 10^{-4}$	59	$3.6 \times 10^{-4}$	39	$6.5 \times 10^{-4}$	72	$8.5 \times 10^{-4}$
4	16	1024	82	$6.7 \times 10^{-4}$	53	$7.0 \times 10^{-3}$	88	$2.5 \times 10^{-4}$	51	$6.7 \times 10^{-4}$	99	$1.8 \times 10^{-3}$
8	32	2048	236	$1.6 \times 10^{-3}$	112	$2.1 \times 10^{-4}$	205	$2.3 \times 10^{-4}$	111	$1.8 \times 10^{-3}$	197	$4.3 \times 10^{-3}$

CFIER and CFIERPS formulations consistently outperform solvers based on the classical formulations CFIEFK<sup>2</sup> and CFIESK in the regime under consideration. Furthermore, the solvers based on the SCFIE and CFIER formulations compare favorably to the solvers based on the CFIESK formulation.

TABLE 9.

$k_1$	$k_2$	X	CFIEFK <sup>2</sup>		CFIESK		SCFIE*		CFIER		CFIERPS	
			Iter.	$\epsilon_\infty$	Iter.	$\epsilon_\infty$	Iter.	$\epsilon_\infty$	Iter.	$\epsilon_\infty$	Iter.	$\epsilon_\infty$
1	4	352	76	$5.4 \times 10^{-4}$	40	$4.8 \times 10^{-3}$	57	$5.5 \times 10^{-3}$	58	$5.1 \times 10^{-4}$	66	$3.5 \times 10^{-4}$
2	8	704	98	$7.7 \times 10^{-4}$	64	$2.0 \times 10^{-3}$	87	$9.6 \times 10^{-4}$	66	$1.9 \times 10^{-4}$	107	$8.1 \times 10^{-4}$
4	16	1408	236	$1.7 \times 10^{-3}$	126	$2.2 \times 10^{-3}$	168	$4.3 \times 10^{-4}$	128	$9.2 \times 10^{-4}$	181	$2.5 \times 10^{-3}$
8	32	2816	424	$3.2 \times 10^{-3}$	252	$2.8 \times 10^{-3}$	286	$7.0 \times 10^{-4}$	216	$1.1 \times 10^{-3}$	305	$3.3 \times 10^{-3}$

TABLE 10.

$k_1$	$k_2$	X	CFIEFK <sup>2</sup>		CFIESK		SCFIE*		CFIER		CFIERPS	
			Iter.	$\epsilon_\infty$	Iter.	$\epsilon_\infty$	Iter.	$\epsilon_\infty$	Iter.	$\epsilon_\infty$	Iter.	$\epsilon_\infty$
3.5	1	256	16	$2.1 \times 10^{-3}$	23	$8.1 \times 10^{-4}$	21	$1.1 \times 10^{-3}$	20	$1.7 \times 10^{-3}$	21	$3.3 \times 10^{-3}$
7	2	512	29	$1.7 \times 10^{-3}$	41	$2.0 \times 10^{-3}$	24	$4.4 \times 10^{-4}$	20	$2.1 \times 10^{-3}$	30	$2.0 \times 10^{-3}$
14	4	1024	59	$8.9 \times 10^{-3}$	56	$1.7 \times 10^{-1}$	35	$3.2 \times 10^{-4}$	22	$1.1 \times 10^{-3}$	57	$4.2 \times 10^{-3}$
28	8	2048	85	$4.1 \times 10^{-2}$	94	$9.4 \times 10^{-2}$	39	$5.5 \times 10^{-4}$	25	$1.1 \times 10^{-3}$	87	$1.2 \times 10^{-2}$

TABLE 11.

$k_1$	$k_2$	X	CFIEFK <sup>2</sup>		CFIESK		SCFIE*		CFIER		CFIERPS	
			Iter.	$\epsilon_\infty$	Iter.	$\epsilon_\infty$	Iter.	$\epsilon_\infty$	Iter.	$\epsilon_\infty$	Iter.	$\epsilon_\infty$
3.5	1	352	42	$3.4 \times 10^{-3}$	51	$2.4 \times 10^{-3}$	30	$3.6 \times 10^{-3}$	26	$1.5 \times 10^{-3}$	37	$2.4 \times 10^{-3}$
7	2	704	54	$3.2 \times 10^{-3}$	70	$2.7 \times 10^{-2}$	35	$3.0 \times 10^{-4}$	33	$1.3 \times 10^{-3}$	47	$2.7 \times 10^{-3}$
14	4	1408	123	$2.7 \times 10^{-2}$	148	$9.5 \times 10^{-2}$	47	$3.2 \times 10^{-4}$	46	$1.2 \times 10^{-3}$	77	$2.6 \times 10^{-3}$
28	8	2816	238	$9.8 \times 10^{-2}$	240	$1.3 \times 10^{-1}$	84	$3.6 \times 10^{-4}$	67	$1.8 \times 10^{-3}$	169	$4.2 \times 10^{-3}$

TABLE 12. Scattering experiments for the  $B_q$ ,  $q = 512$ , sphere of radius 2 with  $\rho = 1$ , and for the CFIEFK<sup>2</sup>, CFIESK, SCFIE and CFIERPS formulations.

$k_1$	$k_2$	X	CFIEFK <sup>2</sup>		CFIESK		SCFIE*		CFIER		CFIERPS	
			Iter.	$\epsilon_\infty$	Iter.	$\epsilon_\infty$	Iter.	$\epsilon_\infty$	Iter.	$\epsilon_\infty$	Iter.	$\epsilon_\infty$
1	4	256	20	$5.0 \times 10^{-3}$	25	$2.7 \times 10^{-4}$	19	$8.7 \times 10^{-3}$	30	$5.8 \times 10^{-3}$	21	$5.8 \times 10^{-3}$
2	8	512	24	$2.8 \times 10^{-3}$	41	$3.7 \times 10^{-4}$	30	$1.4 \times 10^{-3}$	32	$5.6 \times 10^{-3}$	32	$1.7 \times 10^{-3}$
4	16	1024	62	$4.0 \times 10^{-3}$	97	$1.8 \times 10^{-3}$	55	$1.4 \times 10^{-3}$	59	$5.6 \times 10^{-3}$	62	$1.8 \times 10^{-3}$
8	32	2048	122	$7.9 \times 10^{-3}$	173	$5.6 \times 10^{-3}$	96	$3.3 \times 10^{-3}$	103	$8.7 \times 10^{-3}$	117	$4.6 \times 10^{-3}$

We conclude with an illustration in Tables 10–11 of high contrast, high-frequency scenarios whereby the computational gains associated with solvers based on the SCFIE, CFIER and CFIERPS are the most significant. As can be seen in Table 11, solvers based on the SCFIE and CFIER formulations can result in computational times that are at least three times faster than those based on the classical CFIESK and CFIEFK formulations.

Finally, we present in Table 12 a comparison between scattering solutions corresponding to Lipschitz scatterers and solutions corresponding to nearby smooth scatterers that are obtained from rounding the corners. More specifically, we considered the sphere of radius 2 in  $\mathbb{R}^2$  using the  $\ell^q$  norm for  $q = 512$ , that is,

$$B_q := \{(x_1, x_2) \in \mathbb{R}^2 : x_1^q + x_2^q = 2^q\}, \quad q = 512,$$

which is a close and smooth (rounded) approximation of the square geometry in Figure 1; indeed, the distance between the scatterers is about  $10^{-3}$ . We compare the far-field signature of  $B_q$ ,  $q = 512$ , to that of the square for various wavenumbers using the various boundary integral equation formulations considered in this text. We note that, for a given frequency, the numbers of iterations required by boundary integral formulations to reach the same tolerance are roughly the same for the square and its very close smooth (rounded) approximation, see Tables 6 and 12.

**6. Conclusions.** In this work, we have presented high-order Nyström discretizations based on polynomially graded meshes for several boundary integral formulations including certain regularized formulations for Helmholtz transmission problems in domains with corners. We have rigorously proved the well-posedness of some of these formulations and have shown that solvers based on the regularized and on the single integral equations outperform solvers based on commonly used boundary integral equation formulations in the case of high contrast, high-frequency applications. The numerical analysis of these schemes will be the subject of future investigation. Extensions of the regularization scheme used in this paper for the case of multiple dielectric scatterers will also be the subject of future investigation.

**Acknowledgments.** Part of this research was carried out during a short visit of Víctor Domínguez to NJIT.

We want to thank the reviewer for his/her very careful reading and useful comments which helped us to improve the readability and to complement the theoretical results of this paper.

## REFERENCES

1. R.A. Adams and J.J.F. Fournier, *Sobolev spaces*, Pure Appl. Math. **140**, Elsevier/Academic Press, Amsterdam, 2003.
2. A. Anand, J.S. Owall and C. Turc, *Well-conditioned boundary integral equations for two-dimensional sound-hard scattering problems in domains with corners*, J. Integral Equations Appl. **24** (2012), 321–358.
3. X. Antoine and Y. Boubendir, *An integral preconditioner for solving the two-dimensional scattering transmission problem using integral equations*, Int. J. Comp. Math. **85** (2008), 1473–1490.
4. Y. Boubendir, O. Bruno, C. Levaux and C. Turc, *Integral equations requiring small numbers of Krylov-subspace iterations for two-dimensional smooth penetrable scattering problems*, Appl. Numer. Math. **95** (2015), 82–98.
5. Y. Boubendir, V. Domínguez, C. Levaux and C. Turc, *Regularized combined field integral equations for acoustic transmission problems*, SIAM J. Appl. Math. **75** (2015), 929–952.
6. Y. Boubendir and C. Turc, *Wave-number estimates for regularized combined field boundary integral operators in acoustic scattering problems with Neumann boundary conditions*, IMA J. Numer. Anal. **33** (2013), 1176–1225.
7. Y. Boubendir, C. Turc and V. Domínguez, *High-order Nyström discretizations for the solution of integral equation formulations of two-dimensional Helmholtz transmission problems*, IMA J. Numer. Anal. **36** (2016), 463–492.
8. J. Bremer, *On the Nyström discretization of integral equations on planar curves with corners*, Appl. Comp. Harm. Anal. **32** (2012), 45–64.
9. O.P. Bruno, J.S. Owall and C. Turc, *A high-order integral algorithm for highly singular PDE solutions in Lipschitz domains*, Computing **84** (2009), 149–181.
10. A.J. Burton and G.F. Miller, *The application of integral equation methods to the numerical solution of some exterior boundary-value problems*, Proc. Roy. Soc. Lond. **323** (1971), 201–210.
11. X. Claeys, R. Hiptmair and C. Jerez-Hanckes, *Multitrace boundary integral equations*, in *Direct and inverse problems in wave propagation and applications*, Rad. Ser. Comp. Appl. Math., De Gruyter, Berlin, 2013.
12. M. Costabel, *Boundary integral operators on Lipschitz domains: Elementary results*, SIAM J. Math. Anal. **19** (1988), 613–626.
13. M. Costabel and E. Stephan, *A direct boundary integral equation method for transmission problems*, J. Math. Anal. Appl. **106** (1985), 367–413.
14. L. Escauriaza, E.B. Fabes and G. Verchota, *On a regularity theorem for weak solutions to transmission problems with internal Lipschitz boundaries*, Proc. Amer. Math. Soc. **115** (1992), 1069–1076.

15. L Greengard, Kenneth L. Ho and J.-Y. Lee, *A fast direct solver for scattering from periodic structures with multiple material interfaces in two dimensions*, J. Comp. Phys. **258** (2014), 738–751.
16. J. Helsing, *A fast and stable solver for singular integral equations on piecewise smooth curves*, SIAM J. Sci. Comp. **33** (2011), 153–174.
17. J. Helsing and R. Ojala, *Corner singularities for elliptic problems: Integral equations, graded meshes, quadrature, and compressed inverse preconditioning*, J. Comp. Phys. **227** (2008), 8820–8840.
18. R. Hiptmair and C. Jerez-Hanckes, *Multiple traces boundary integral formulation for Helmholtz transmission problems*, Adv. Comp. Math. **37** (2012), 39–91.
19. K.L. Ho and L. Greengard, *A fast semidirect least squares algorithm for hierarchically block separable matrices*, SIAM J. Matrix Anal. Appl. **35** (2014), 725–748.
20. R. Kittappa and R.E. Kleinman, *Acoustic scattering by penetrable homogeneous objects*, J. Math. Phys. **16** (1975), 421–432.
21. R.E. Kleinman and P.A. Martin, *On single integral equations for the transmission problem of acoustics*, SIAM J. Appl. Math. **48** (1988), 307–325.
22. R. Kress, *A Nyström method for boundary integral equations in domains with corners*, Numer. Math. **58** (1990), 145–161.
23. ———, *On the numerical solution of a hypersingular integral equation in scattering theory*, J. Comp. Appl. Math. **61** (1995), 345–360.
24. ———, *Linear integral equations*, Appl. Math. Sci. **82**, Springer-Verlag, New York, 1999.
25. R. Kress and G.F. Roach, *Transmission problems for the Helmholtz equation*, J. Math. Phys. **19** (1978), 1433–1437.
26. R. Kussmaul, *Ein numerisches Verfahren zur Lösung des Neumannschen Neumannschen Aussenraumproblems für die Helmholtzsche Schwingungsgleichung*, Computing **4** (1969), 246–273.
27. A.R. Laliena, M.-L. Rapún and F.-J. Sayas, *Symmetric boundary integral formulations for Helmholtz transmission problems*, Appl. Numer. Math. **59** (2009), 2814–2823.
28. W. Lu and Y.Y. Lu, *Efficient high order waveguide mode solvers based on boundary integral equations*, J. Comp. Phys. **272** (2014), 507–525.
29. E. Martensen, *Über eine Methode zum räumlichen Neumannschen Problem mit einer Anwendung für torusartige Berandungen*, Acta Math. **109** (1963), 75–135.
30. W. McLean, *Strongly elliptic systems and boundary integral equations*, Cambridge University Press, Cambridge, 2000.

**31.** G. Monegato and L. Scuderi, *A polynomial collocation method for the numerical solution of weakly singular and nonsingular integral equations on non-smooth boundaries*, Int. J. Numer. Meth. Eng. **58** (2003), 1985–2011.

**32.** M.-L. Rapún and F.-J. Sayas, *Boundary integral approximation of a heat-diffusion problem in time-harmonic regime*, Numer. Algor. **41** (2006), 127–160.

**33.** ———, *Mixed boundary integral methods for Helmholtz transmission problems*, J. Comp. Appl. Math. **214** (2008), 238–258.

**34.** V. Rokhlin, *Solution of acoustic scattering problems by means of second kind integral equations*, Wave Motion **5** (1983), 257–272.

**35.** Y. Saad and M.H. Schultz, *GMRES: A generalized minimal residual algorithm for solving nonsymmetric linear systems*, SIAM J. Sci. Stat. Comp. **7** (1986), 856–869.

**36.** R.H. Torres and G.V. Welland, *The Helmholtz equation and transmission problems with Lipschitz interfaces*, Indiana Univ. Math. J. **42** (1993), 1457–1485.

**37.** G. Verchota, *Layer potentials and regularity for the Dirichlet problem for Laplace's equation in Lipschitz domains*, J. Funct. Anal. **59** (1984), 572–611.

**38.** T. von Petersdorff, *Boundary integral equations for mixed Dirichlet, Neumann and transmission problems*, Math. Meth. Appl. Sci. **11** (1989), 185–213.

DEP. INGENIERÍA MATEMÁTICA E INFORMÁTICA, UNIVERSIDAD PÚBLICA DE NAVARRA, CAMPUS DE TUDELA 31500-TUDELA, SPAIN AND INSTITUTE FOR ADVANCED MATERIALS (INAMAT), 31006 PAMPLONA, SPAIN

**Email address:** [victor.dominguez@unavarra.es](mailto:victor.dominguez@unavarra.es)

DEPARTMENT OF MATHEMATICS AND STATISTICS, UNIVERSITY OF NEW HAMPSHIRE, DURHAM, NH 03861

**Email address:** [mark.lyon@unh.edu](mailto:mark.lyon@unh.edu)

DEPARTMENT OF MATHEMATICAL SCIENCES AND CENTER FOR APPLIED MATHEMATICS AND STATISTICS, NEW JERSEY INSTITUTE OF TECHNOLOGY, UNIV. HEIGHTS. 323, DR. M.L. KING JR. BLVD., NEWARK, NJ 07102

**Email address:** [catalin.c.turc@njit.edu](mailto:catalin.c.turc@njit.edu)